

Universidade de Lisboa
Faculdade de Medicina da Universidade de Lisboa



**Diffuse low grade gliomas with
secondary malignancy
Immunohistochemical and Cytogenetic
profile study**

Mariana Cunha Barbosa

Orientadores: Professor Doutor José Pimentel e Mestre Pedro Pereira

**Dissertação especialmente elaborada para obtenção do
grau de Mestre em Oncobiologia**

2019

Universidade de Lisboa
Faculdade de Medicina da Universidade de Lisboa



**Diffuse low grade gliomas with
secondary malignancy
Immunohistochemical and Cytogenetic
profile study**

Mariana Cunha Barbosa

Orientadores: Professor Doutor José Pimentel e Mestre Pedro Pereira

**Dissertação especialmente elaborada para obtenção do
grau de Mestre em Oncobiologia**

2019

**A impressão desta dissertação foi aprovada pelo Conselho Científico
da Faculdade de Medicina de Lisboa em reunião de 15 de janeiro de
2019**

“Wit beyond measure is man’s greatest treasure.”

— J.K. Rowling, *Harry Potter and the Order of the Phoenix*

Agradecimentos

Ao meu orientador, Professor Doutor José Pimentel, e co-orientador, Mestre Pedro Pereira, pela disponibilidade demonstrada em todos os momentos, pelo apoio científico e incentivo moral que me deram ao longo de todo este trabalho;

Ao laboratório do Professor Doutor Luís Costa e à Doutora Sandra Casimiro pela ajuda prestada na disponibilização de sondas de FISH;

À minha família, que me ensinou a sonhar alto e a trabalhar com dedicação e “amor à camisola”, e que nunca me deixou desmotivar, mesmo com todos os percalços que encontrei no caminho;

À minha amiga, Miriam Gomes, que me apoiou desde o planeamento, à prática e até à revisão desta dissertação, por todas as horas que passou a ouvir-me, e pela ajuda que me deu para que me mantivesse optimista, quando eu não o conseguia sozinha, e realista, quando duvidava de mim própria;

À Sara Marques, pelo entusiasmo contagiante que me ajudou a chegar ao fim, pela partilha de experiências e sentimentos durante todo o processo, e por toda a ajuda científica que me deu;

Por fim, ao João, meu namorado e companheiro de todas as alturas, que se manteve sempre ao meu lado sem vacilar, que soube lidar com todas as minhas fases e nunca demonstrou menos do que orgulho neste meu percurso;

A todos os que se cruzaram comigo nesta etapa que foi tão longa e desesperante como maravilhosa e emocionante,

Um grande “Muito Obrigada”.

Resumo

Os gliomas são os tumores primários mais frequentes do Sistema Nervoso Central, representando 50% de todos os casos de tumores cerebrais. Incluem, entre outros, os astrocitomas (AT) e os oligodendrogliomas (OLG).

Uma designação comum para estes tumores, quando se localizam num ou mais lobos cerebrais, na região supratentorial é a de gliomas difusos e atingem, caracteristicamente, jovens adultos. Esses dois tipos de gliomas são considerados de baixo grau e são infiltrativos, de crescimento lento. Os gliomas de baixo grau – grau II, pela Organização Mundial de Saúde – tem uma forte tendência para a progressão maligna, para gliomas anaplásicos (grau III, pela OMS) e até glioblastomas secundários (grau IV, pela OMS), o que, muitas vezes, ocorre após alguns anos, geralmente, entre cerca de 4 a 5.

Muitas vezes, após uma ressecção cirúrgica de gliomas de baixo grau, as células neoplásicas deixadas no cérebro podem originar um tumor recidivante, que muitas vezes se transforma em glioma de alto grau, com prognóstico variável a longo prazo e uma taxa de sobrevida de entre 5 a 8 anos.

A nova classificação da OMS, no que diz respeito a Tumores do Sistema Nervoso Central, revista em 2016, introduziu parâmetros moleculares como mutações *IDH*, co-deleções de *1p/19q* e perdas de *ATRX*, agrupando os tumores em categorias de acordo com seus perfis genéticos, além dos padrões histológicos usados até então.

Sendo assim, é possível classificar os gliomas difusos em astrocitomas, *IDH* mutantes; oligodendrogliomas, *IDH* mutantes e *1p/19q* co-deletados; astrocitomas *IDH wild-type*; glioblastomas *IDH* mutantes; glioblastomas *IDH wild-type*; oligodendrogliomas sem outras especificações; astrocitomas sem outras especificações; oligoastrocitomas sem outras especificações e glioblastomas sem outras especificações.

Os critérios usados para definir o grau de anaplasia dos gliomas, definidos pela OMS, são polimorfismo nuclear e hipercromasia, índice mitótico, proliferação endotelial da microvascularização tumoral e necrose do parênquima tumoral. Estes critérios permitem aos patologistas classificar os gliomas difusos em diferentes graus de malignidade, desde grau II, o menos maligno, até aos graus III e IV, os mais malignos, dos quais o glioblastoma é o mais comum.

As alterações moleculares no processo de tumorigénese levam à ativação de oncogenes ou à inativação de genes supressores de tumor.

Alguns dos marcadores genéticos de grande relevância no processo de tumorigénese e na determinação do tipo e grau de anaplasia dos gliomas difusos são o *1p/19q* (co-deleção), o *EGFR*, o *PTEN* e o *CDKN2A*.

A presença de mutação do *ATRX* ajuda ao diagnóstico dos AT com *IDH* mutante, distinguindo-os dos OLG. Os AT anaplásicos com mutações combinadas no *ATRX* e no *IDH* têm melhor prognóstico do que os que só têm a mutação do *IDH*.

As mutações no codão 132 do gene *IDH* ocorrem cedo e a uma frequência elevada em AT, OLG de graus II e III, e em glioblastomas secundários desenvolvidos a partir de AT.

Os objetivos deste estudo são comparar o perfil imunohistoquímico e as alterações citogenéticas encontradas em 16 casos de doentes com cirurgia a gliomas primários de baixo grau, e a recidiva de grau mais elevado, resultando num total de 32 amostras – 18 oligodendrogliomas, 10 astrocitomas, 3 oligoastrocitomas e 1 gliossarcoma; avaliar e quantificar as alterações e identificar subpopulações baseadas em marcadores, nas amostras de tumores de ambas as cirurgias.

Para isso, obtiveram-se lâminas de imunohistoquímica e fizeram-se blocos de *Tissue Micro Arrays*, dos quais se obtiveram lâminas para Hibridação *In Situ* por Fluorescência.

As proteínas estudadas foram *GFAP*, *IDH1*, *KI-67*, *ATRX* e *Olig-2*, e os genes foram *CDKN2A*, *p53*, *EGFR*, *PTEN*, *1p* e *19q*.

Realizou-se a técnica de imunohistoquímica para os marcadores *IDH*, *ATRX* e *GFAP*, posteriormente fotografados no microscópio ótico, e analisados com programa *Image-J* (plugin *Colour Deconvolution*). Às áreas de interesse foram-lhes atribuídas cores secundárias (cada uma associada a um marcador) e as imagens resultantes foram sobrepostas originando áreas de cores primárias. Foi calculado o rácio de *pixéis* de cada cor de interesse. Realizou-se igualmente a técnica de imunohistoquímica para os marcadores *Olig-2* e *KI-67*, também fotografados no microscópio ótico e analisados no programa *Image-J* (plugin *ImmunoRatio*).

Realizou-se ainda Hibridação *in situ* de fluorescência, para analisar os genes *CDKN2A*, *p53*, *EGFR*, *PTEN*, *1p* e *19q*, em lâminas de *Tissue Micro Array*, que foram fotografadas no microscópio de fluorescência e analisadas no programa *Image-J* (plugin *Cell Counter* para contagem dos núcleos).

Este estudo incluiu 18 oligodendrogliomas, 10 astrocitomas, 3 oligoastrocitomas e 1 gliossarcoma.

A análise foi feita inicialmente para os marcadores individuais e, em seguida, para as subpopulações definidas, baseadas na classificação actual de gliomas difusos.

Nenhuma das amostras estudadas apresentou deleção do gene supressor tumoral *PTEN*.

O estudo de *EGFR* mostrou amplificação em apenas 6 das 32 amostras, sendo 4 exclusivamente nas recidivas e 1 exclusivamente num tumor primário de baixo grau.

O *p53* estava mutado em 6 das 32 amostras estudadas, sendo que 4 desses 6 tumores com mutação eram recidivas. Analisando as alterações de primários para recidivas, encontraram-se 4 casos com *p53 wild-type* no primário e mutação nas recidivas e 1 caso que manteve a mutação em ambos os grupos.

O *CDKN2A* estava deletado no primário e na recidiva em simultâneo, em apenas 1 caso. 6 casos tinham deleções nos primários e apenas 3 tinham deleções nas recidivas.

A expressão de *KI-67* apresentou valores mais elevados nas recidivas do que nos primários.

Relativamente à expressão de *Olig-2*, observou-se o contrário, sendo os valores mais elevados nos primários do que nas recidivas.

Não se encontraram diferenças *major* nas três subpopulações estudadas (*IDH1mut/ATRXloss*, *IDH1mut/ATRX/1p/19q* co-deletadas e *IDH1wt*) entre as amostras de tumores primários e as suas respectivas recidivas.

Descobriram-se mais células tumorais *IDH1mut/ATRXloss* em recidivas (9799 ± 24384) do que em primários (5053 ± 10116), e mais células tumorais *IDH1-* em primários (671939 ± 180448) do que nas recidivas (609653 ± 284091). Contudo, estas diferenças não foram muito evidentes.

Células *IDH1mut/ATRX/1p/19q* co-deletadas foram encontradas em apenas um dos dezasseis casos estudados.

As proteínas e genes estudados cobrem a maioria das principais vias de sinalização molecular que levam ao desenvolvimento de carcinomas. Contudo, a ausência de variações muito evidentes entre os dois grupos comparados (primário e respetiva recidiva) indica que poder-se-á não estar a estudar os marcadores mais relevantes para esta evolução.

Outros marcadores que poderão ser relevantes são o *PDGF* e o *Ras*.

O *PDGF* é um agente mitogénico de células mesenquimais, incluindo células gliais e já foi associado a glioblastomas (vias *PI3k/AKT* e *Ras-Raf-Mek-Erk*). O gene *Ras* foi o primeiro oncogene humano a ser identificado e sabe-se que está mutado em cerca de um terço dos carcinomas. Estes são apenas dois exemplos de outras moléculas que podem ser estudadas nos gliomas.

Este estudo é um passo noutra direcção, no que diz respeito aos marcadores biológicos em gliomas. Os resultados obtidos levantam variadas questões face aos marcadores estudados e oferecem uma série de sugestões de outros a considerar; e, uma vez que não há bibliografia de suporte, seria interessante continuar a estudar esta linha de progressão tumoral do primário para a recidiva. O objetivo não seria apenas caracterizar subgrupos histológicos de gliomas do ponto de vista genético e molecular mas também, e acima de tudo, tentar compreender a evolução do tumor primário e os mecanismos e ferramentas biológicas presentes no próprio, que lhe permite recidivar com um nível de malignidade superior. Se se conseguir prever estas transformações no tempo, poder-se-á tentar controlar a progressão da doença logo desde o momento do diagnóstico.

Abstract

The most frequent primary tumors of the Central Nervous System are gliomas, representing 50% of all brain tumor cases, which include, among others, astrocytomas and oligodendrogliomas.

Those two types of gliomas, considered low-grade gliomas, are infiltrative and slow-growing. Low-grade gliomas (World Health Organization grade II) have a strong tendency for malignant progression to anaplastic gliomas (World Health Organization grade III) and even secondary glioblastomas (World Health Organization grade IV), which often takes place after a few years, usually about 4 to 5.

Indeed, after a surgical resection of LGG, cancerous cells left in the brain can give rise to a recurrent tumor, often transformed in a high-grade glioma, with variable long-term prognoses and a survival rate between 5 to 8 years.

The new World Health Organization Classification of Tumors of the Central Nervous System, revised in 2016, introduced molecular parameters, such as *IDH* mutations, *1p/19q* co-deletions and *ATRX* losses, for grouping tumors into categories according to their genetic profiles besides the histologic patterns used until then.

The aim of this study is to compare immunohistochemical profile and cytogenetic changes in 16 cases with two different surgeries from the same patient, treated for recurrences, evaluate and quantify those changes and identify marker based subpopulations in tumour samples from both surgeries. The proteins studied were *GFAP*, *IDH1*, *KI-67*, *ATRX* and *Olig-2*, and the genes were *CDKN2A*, *p53*, *EGFR*, *PTEN*, *1p* and *19q*.

We did not find major differences in the populations we studied (*IDH1mut/ATRXloss*, *IDH1mut/ATRX/1p/19q* co-del and *IDH1wt*) between primaries and their relapses.

However, differences were found in *Ki-67*, *Olig-2*, *EGFR* and *CDKN2A* between the two groups studied (primary tumors and relapses).

All proteins and genes studied cover most of the main pathways that lead to cancer development, which may lead us to think that we are looking at the wrong set of markers.

We found some results that suggest it should be interesting to continue this type of research of comparing primary tumors with their own relapses, and try to understand what makes tumors relapse in a much more aggressive form, in order to control the progression of the disease right in the moment of the diagnosis.

Keywords: low-grade gliomas; subpopulations; primary tumors, relapse tumors, FISH, IHQ

Abbreviations

AAT – Anaplastic Astrocytoma
ALT – Alternative Lengthening Telomeres
AOLG – Anaplastic Oligodendroglioma
AT – Astrocytomas
ATRX – α -Thalassemia/Mental Retardation Syndrome X-linked
CNS – Central Nervous System
DAB – 3,3'-diaminobenzidine
DAPI – 4',6-Diamidino-2-phenylindole
DG – Diffuse Gliomas
DNA – Deoxyribonucleic Acid
EGFR – Epidermal Growth Factor Receptor
FISH – Fluorescence *In Situ* Hybridization
GB – Glioblastoma
GFAP - Glial Fibrillary Acidic Protein
GS – Gliosarcoma
IDH – Isocitrate dehydrogenase
IHC – Immunohistochemistry/ Immunohistochemical
LGG – Low-Grade Glioma
LN – Laboratory of Neuropathology
NOS – No Other Specification
OLG – Oligodendrogliomas
OLGA – Oligoastrocytomas
ON – Overnight
PBS – Phosphate Buffered Saline
PML – Pro Myelocytic Leukemia
PTEN – Phosphatase and Tensin Homolog
RGB – Red, Green, Blue
RT – Room Temperature
SG-B – Secondary Glioblastoma
SNF2 – SWItch/Sucrose Non-Fermentable2
TMA – Tissue Micro Arrays
WHO – World Health Organization
WT – Wild Type
 μm – Micrometre

Table of Contents

Agradecimientos	iiiv
Resumo	v
Abstract	viii
Abbreviations	ix
1. Introduction	14
1.1 Diffuse Gliomas	14
1.2 Gene and Protein Expressions	14
2. Objectives.....	22
3. Ethical Considerations.....	23
4. Material and Methods.....	24
4.1 Sampling Method.....	24
4.2 Immunohistochemistry	25
4.3 Fluorescent <i>In Situ</i> Hybridization	25
4.4 Data Analysis	26
4.4.1 ATRX, IDH1 and GFAP	26
4.4.2 Olig-2 and KI-67	28
4.4.3 FISH	29
4.4.4 Statistics	29
5. Results	30
6. Discussion and conclusions.....	48
7. References	52
8. Appendixes.....	60

Figure Index

Figure 1 - A simplified algorithm for classification of the diffuse gliomas, 2016 CNS WHO [4]	15
Figure 2- Neomorphic enzyme activity of mutant <i>IDH</i> enzymes. <i>IDH1</i> and <i>IDH2</i> catalyse the oxidative decarboxylation of isocitrate to generate α KG, using NADP ⁺ as a cofactor and producing NADPH and CO ₂ . Recurrent mutations in the active site of <i>IDH1</i> and <i>IDH2</i> confer a gain of function activity that catalyses the conversion of α KG into D2HG in a manner that consumes NADPH. [18].	16
Figure 3 – <i>ATRX</i> from PML bodies and ribosomal DNA remodelling chromatin through the consumption of ATP. [30].	18
Figure 4- Sampling criteria	24
Figure 5 - RGB and primary colour scheme used in Image-J analysis	26
Figure 6 - On top: Photographs from the IHC slides of one of the cases. Bellow: The isolation of the brown areas (expression of antibodies), converted in black. (From left to right: GFAP, <i>IDH1</i> and <i>ATRX</i>)	27
Figure 7 - Overlap of two different antibodies (<i>GFAP</i> and <i>ATRX</i>) through the attribution of primary s to the stained areas. (<i>GFAP</i> - blue; <i>ATRX</i> - Green; Overlap - Cyan)	27
Figure 8 - Example of the application of the plugin ImmunoRatio in a sample slide stained for <i>KI-67</i> . Three distinct fields where photographed and the ratio between stained nuclei and non-stained nuclei were obtained. On top are the original photographs and at the bottom are the nuclei considered to the calculation.	28
Figure 9 - Example of the evolution of <i>KI-67</i> from primary tumor sample (top images) to relapse tumor sample (bottom images). Three fields of each slide were photographed and the DAB/Nuclear area average ratios found were: Primary tumor sample – 3,4% and Relapse tumor sample – 8,6%.	30
Figure 10 - Evolution of the expression of individual markers from primary tumors to their relapses.	31
Figure 11 - Example of the evolution of <i>Olig-2</i> from primary tumor sample (top images) to relapse tumor sample (bottom images). Three fields of each slide were photographed and the DAB/Nuclear area average ratios found were: Primary tumor sample – 84,3% and Relapse tumor sample – 50,7%.	31
Figure 12 - Evolution of the expression of individual markers from primary tumors to their relapses.	32
Figure 13 - Evolution of the expression of individual markers from primary tumors to their relapses.	32

Figure 14- Illustration of the layered analysis performed in the samples showing the colocalization spots of two antibodies, which represent subpopulations of cells with different protein expressions.....	33
Figure 15- Tumor Subpopulations of cells studied.	34
Figure 16 – Comparison of mean values of subpopulations of tumor cells from primary tumors to their relapses.	35
Figure 17 - Comparison of mean values of subpopulations of tumor cells from primary tumors to their relapses.	36
Figure 18- Comparison of mean values of subpopulations of tumor cells among different groups based in histomorphological diagnosis.	39
Figure 19- Variations found in <i>EGFR</i> , increase in amplification from primary tumor samples to relapses.....	42
Figure 20 - Variations found in <i>EGFR</i> , decrease in amplification from primary tumor samples to relapses.....	44
Figure 21 - <i>p53</i> mutations found in primary tumor samples and relapses.	45
Figure 22 - Percentage of <i>CDKN2A</i> deletions in primary tumor samples vs. relapses.....	46
Figure 23 - FISH results for <i>CDKN2A</i> deletion.	46
Figure 24 - Three lines of mutations-based tumors.....	48

Table Index

Table 1 - Image-J table of coloured Areas.	28
Table 2 - Type of mutation by gene	29
Table 3- Proportion of samples in the study divided by histological classification	30
Table 4 – Formulas used for the calculation of areas	34
Table 5 - <i>IDH1</i> + <i>ATRX</i> +, <i>1p19q</i> co-deleted subpopulations.....	37
Table 6 - <i>EGFR</i> FISH positive results.	42
Table 7 - <i>p53</i> mutations.....	44
Table 8 - Summary of differences found in markers studied between primary tumors and relapse tumors.....	47

1.1 Diffuse Gliomas

Central Nervous System (CNS) primary tumors account for 2% of all tumors and are associated with high mortality rates, being one of the most devastating cancers. These tumors often show locally aggressive behaviour and cannot be cured by recurrent therapies.[1,2] The most frequent are gliomas, representing 50% of all brain tumor cases, which include, among others, astrocytomas (AT) and oligodendrogliomas (OLG).[1,2]

A common designation for these tumors when located on one or more cerebral lobes, on the supratentorial floor, is diffuse gliomas (DG), characteristically affecting younger adults.

Until the last revision of the World Health Organization (WHO), their pathological classification was centred on the histomorphological characteristics, based on the resemblance of their cells with normal glial cells tissue of origin, complemented by immunohistochemistry techniques (IHC).[1,2]

Those two types of gliomas considered low-grade gliomas (LGG) are infiltrative and slow-growing. LGG (WHO grade II) have a strong tendency for malignant progression to anaplastic gliomas (WHO grade III) and even secondary glioblastomas (WHO grade IV), which often takes place after a few years, usually about 4 to 5.[3] Indeed, after a first surgical resection of LGG, the cancerous cells left in the brain can give rise to a recurrent tumor, often transformed in high-grade glioma, with variable long-term prognoses and survival rates between 5 to 8 years.[4]

The new WHO Classification of Tumors of the CNS, revised in 2016, introduced molecular parameters, such as *IDH* mutations, *1p/19q* co-deletions and *ATRX* losses, grouping tumors into categories according to their genetic profile besides histologic patterns, as shown in Figure 1.[4] Therefore, we can classify DG into Diffuse AT, *IDH* mutant; OLG, *IDH* mutant and *1p/19q* co-deleted; Diffuse AT *IDH-1* wild-type; Glioblastoma (GB), *IDH* mutant; GB *IDH* wild-type; OLG, No other specification (NOS); AT, NOS; Oligoastrocytomas (OLGA), NOS and GB, NOS (Figure 1).[4]

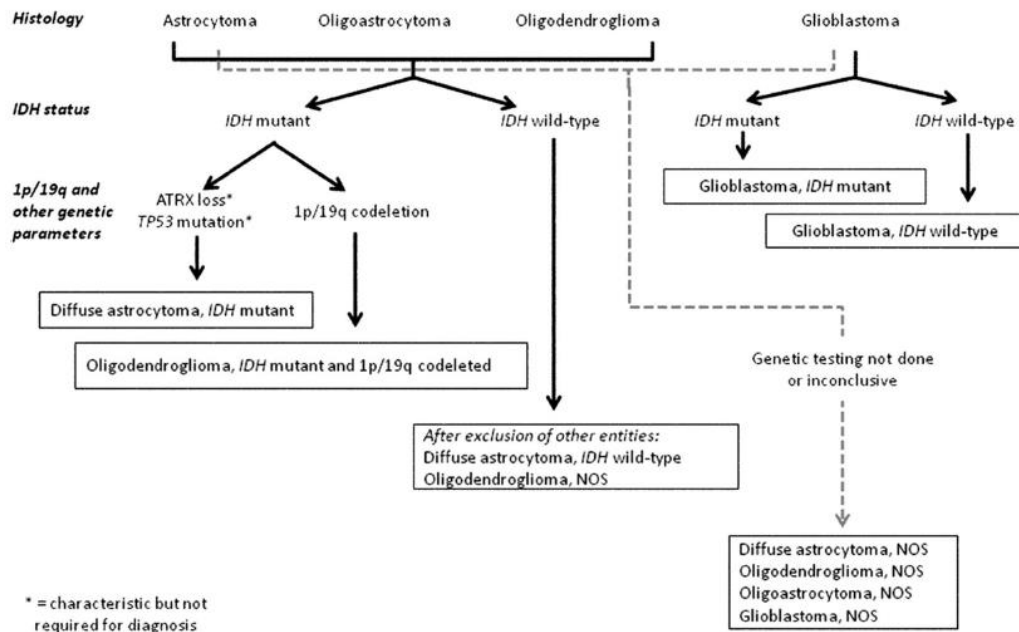


Figure 1 - A simplified algorithm for classification of the diffuse gliomas, 2016 CNS WHO [4]

Histological criteria used for grading DG anaplasia, as defined by WHO, are nuclear polymorphism and hyperchromasia, mitotic index, endothelial proliferation of tumor microvascularisation vessels and tumor parenchyma necrosis. These criteria allow pathologists to classify DG into different degrees of malignancy, from II, the most benign, to III and IV, the most malignant, of which GB is the most common.[2,3]

Molecular criteria with prognostic value, in addition to histological ones, includes several markers [4] among which, *ATRX* and *IDH* (mutation r132) are two of the most used in neuropathological diagnosis.[5-7]

1.2 Gene and Protein Expressions

Molecular alterations occurring during tumorigenesis lead to oncogene activation or tumor suppressor gene inactivation.

Some genetic markers with great relevance in tumorigenesis and in determining type and degree of DG anaplasia are *1p19q* (co-deletion), *EGFR*, *PTEN* and *CDKN2A*. [8]

Korshunov et al. have successfully used Fluorescent *In Situ* Hybridization (FISH) probes for these markers to obtain clinically useful information for 114 high-grade gliomas, morphologically ambiguous, composed of small cells.[9] Another study, performed to detect only *PTEN* and *EGFR*, including tissue samples confirmed by

biopsy of 63 cases of anaplastic astrocytoma (AAT) and 111 cases of glioblastoma multiform, demonstrated clinical significance of these markers.[10]

The presence of mutated *ATRX* helps the diagnosis of AT with an *IDH* mutation, distinguishing them from OLG. Anaplastic AT with combined *ATRX* and *IDH* mutations has better prognosis than those with only *IDH* mutation.[5] Mutations at codon 132 of the *IDH* gene occur early and with a high frequency in AT and OLG grades II and III, and in secondary GB developed from AT.[5]

1.2.1 *IDH*

In 2008, a multi-group collaboration sequenced over 20,000 genes in 22 GB and identified a common point mutation in *IDH1* in 12% of the analysed samples.[11] Further studies found that this mutation is present in 80% of grade II-III gliomas and secondary GB.[9-11] Mutations in *IDH2* have also been identified in gliomas, although they are much less common and mutually exclusive with *IDH1* mutations.[9, 12, 13] Also, *IDH1* is detectable by IHC techniques, or gene sequencing, when negative or any other justified cases, which make this protein suitable for diagnosis routine.

All mutations identified until now have a single amino-acid missense mutation in *IDH1* at arginine 132 (R132) or the analogous residue in *IDH2* (R172). This residue is located at the enzyme active site and is critical for isocitrate binding.[17] Before these observations, mutation of *IDH* genes had never been linked to cancer.[15]

Isocitrate dehydrogenase 1 (*IDH1*) catalyses the oxidative decarboxylation of isocitrate to 2-oxoglutarate (Figure 2).

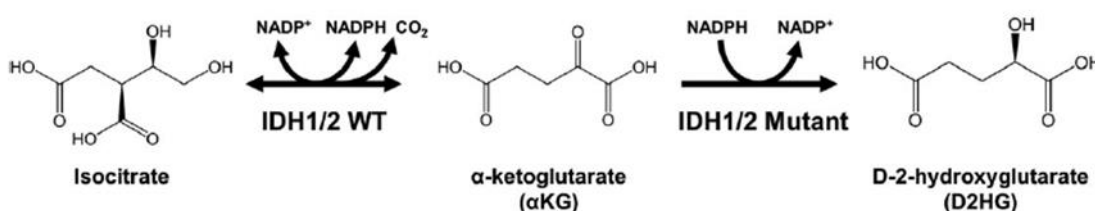


Figure 2- Neomorphic enzyme activity of mutant *IDH* enzymes. *IDH1* and *IDH2* catalyse the oxidative decarboxylation of isocitrate to generate α KG, using NADP^+ as a cofactor and producing NADPH and CO_2 . Recurrent mutations in the active site of *IDH1* and *IDH2* confer a gain of function activity that catalyzes the conversion of α KG into D2HG in a manner that consumes NADPH. [18]

The mutation at R132 inactivates the protein's ability to bind isocitrate and abolishes its normal catalytic activity. This results in reduced levels of α -KG and NADPH, important

cofactor necessary to maintain normal levels of reduced glutathione to combat reactive oxygen species.[15-16] Somatic mosaicism for *IDH1* or *IDH2* at R132 causes enchondromatosis syndromes, Ollier's disease and Maffucci syndrome, which are characterized by haemangiomas and cartilaginous tumors, which carry an increased risk for gliomas.[21] Also, introducing of mutated IDH into normal cells causes increased proliferation, increased colony formation, and inability to differentiate.[22]

1.2.2 ATRX

ATRX gene was first discovered through a study of the X-linked mental retardation (MR) syndrome (*ATRX* syndrome) with patients presenting α -thalassemia, severe psychomotor impairments, urogenital abnormalities, and patterns of characteristic facial dimorphism.[23]

ATRX protein exists in two isoforms (180 and 280 kDa) and is highly enriched at GC-rich and repetitive sequences.[24,25] The C-terminus of *ATRX* protein harbors an helicase/ATPase domain, classifying *ATRX* as part of SNF2 (SWItch/Sucrose Non-Fermentable 2) family of chromatin-remodelling proteins.[26]

Further confirming the *ATRX* function as a regulator of chromatin remodelling and transcription is evidence of the formation of an ATP-dependent complex with transcription cofactor DAXX. In addition, *ATRX* also alters the DNase I digestion pattern and triple helix displacement activity.[27]

ATRX has been found at pericentromeric heterochromatin, ribosomal DNA arrays on acrocentric chromosomes, telomeres and Pro Myelocytic Leukemia (PML) nuclear bodies within mouse and human cells.[27-29] Consequently, *ATRX* plays a key role in gene expression regulation and therefore in cancer (Figure 3).[28]

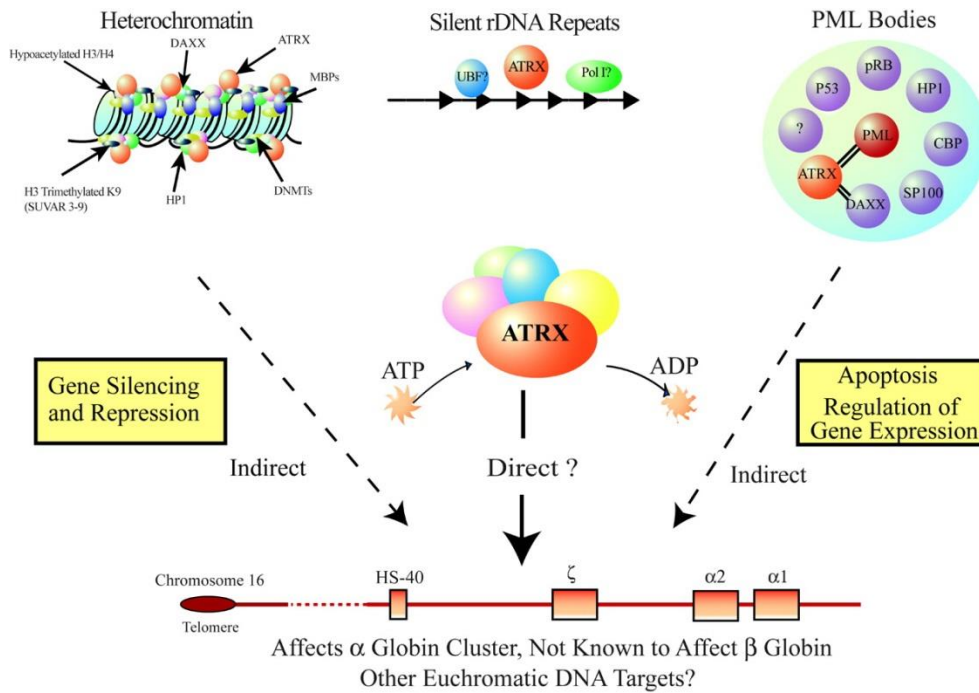


Figure 3 – *ATRX* from PML bodies and ribosomal DNA remodelling chromatin through the consumption of ATP. [30]

ATRX inactivation within gliomas can be due to mutations, deletions, gene fusions or a mix of these causes.[31] Ikemura et al. have demonstrated viability of detecting *ATRX* protein expression using IHC and correlating these expression levels with mutation status, which simplifies the incorporation of *ATRX* analysis in clinical practice.[31] Nowadays, IHC analysis of *ATRX* is determinant in diagnosis and is currently a practice in most places, although genetic sequencing is also performed in some laboratories. Furthermore, *ATRX* mutations correlate with other prominent features, including Alternative Lengthening of Telomeres (ALT) phenotype, TP53 mutations, and occur most often in astrocytic tumors. Interestingly, Kannan et al. [32] reported that within their cohort, mutations related to *ATRX* cofactor DAXX were not found in LGGs and therefore in these tumors, interactions with histone is not as important perhaps.

1.2.3 1p19q

Specific gene mutations, loss of heterozygosity, deletions and/or amplifications of entire chromosomal regions were described in specific tumours including gliomas. Gliomas are characterized particularly by chromosomal deletions, inappropriately activated intracellular signalling pathways, and/or activity loss of tumour suppressor proteins.[35-36] Co-deletion of chromosome 1p/19q is the main loss of heterozygosity studied in gliomas and is associated with a good prognosis and increased responsiveness to

chemotherapy. High incidence of *1p* and *19q* deletion is observed in OLG and OLGA [35] and *1p36-19q13* deletions are closely associated with typical OLG histology, a longer progression-free time and longer median survival time, thus representing an independent prognostic factor in Anaplastic OLG (AOLG) tumors (WHO grade III).[36-37]

This genetic aberration was identified in 1994 and became the first biomarker in neuro-oncology. [35]

Boots-Sprenger, S. et al detected complete *1p/19q* co-deletion in 34% of low-grade gliomas, 52% of anaplastic gliomas and 3% of glioblastomas, and confirmed again that patients with low-grade or anaplastic gliomas with complete *1p/19q* co-deletion were associated to a significant survival benefit.[38]

Wharton, et al. also detected *1p* and *19q* in most of the samples classified as OLG, either WHO grade II or III. [39]

1.2.4 EGFR

EGFR was the first discovered epidermal growth factor receptor, also known as *ErbB-1*. Many cancers have been associated with upregulation of *EGFR* and its overexpression has been identified in the majority of solid tumors, including gliomas.[40] While normal cells express 40,000 to 100,000 *EGFR* receptors, cancer cells may express up to 2,000,000 receptors.[40] Stimulation of overexpressed *EGFR* receptors may contribute to cancer-cell proliferation while simultaneously blocking apoptosis, activating invasion and stimulating tumor-induced neovascularization. The degree of overexpression correlates with tumor progression, resistance to chemotherapy and poor prognosis.[40]

EGFR gene amplification and overexpression are rare in low-grade gliomas but are very typical in GB, being its most common mutant named *EGFRvIII*. [43-44] *EGFRvIII* is unable to bind its ligand due to a deletion of 267 amino-acids from the receptor extracellular domain, making it signal constitutively. The wild-type (WT) receptor is usually co-expressed with the mutated form in GB [44-45] but there are a number of studies [46-47] demonstrating that the mutated form is more tumorigenic than its WT receptor, suggesting *EGFRvIII* signalling plays a key role in gliomagenesis. [41] This increased expression may influence multiple aspects of tumor biology, such as survival, cell proliferation, motility and invasiveness, and even resistance to treatments.[45-46]

1.2.5 PTEN

PTEN was identified in 1997 as a tumor-suppressor gene, by Li et al.[47]

The homologous phosphatase and tensin gene (*PTEN*) mutation in chromosome 10q23 is detected in a wide variety of human cancers, with a frequency comparable to the one of *p53* gene.[48] Both these proteins are tumor suppressors. *PTEN* encodes a lipid phosphatase pathway that negatively regulates phosphoinositol-3-kinase/Akt.[49] The loss of alleles in chromosome 10q is one of the most observed in gliomas.[50]

A *PTEN* FISH study with 217 samples from astrocytoma with diffuse infiltration regions showed significant correlation with histological grade. Clinical results corroborated the usefulness of associating histological interpretation with molecular biology.[51]

PTEN protein–protein interactions can also affect its tumour suppressor properties.[52] In last year's paper, Benitez, J. et al reported a novel chromatin-associated function of *PTEN* tumour suppressor that represses oncogene expression and tumour growth in patient-derived glioma xenografts through DAXX-H3.3 association. They show that DAXX physically interacts with *PTEN*, and *PTEN* regulates H3.3 loading on chromatin by limiting DAXX interactions with this histone, and thereby controls expression of several tumour-promoting genes.[52]

Also, Shen, W. et al demonstrated *PTEN*'s essential role in chromosomal stability maintenance, through physical interaction with centromeres and control of DNA, preventing double-strand breaks.[53]

1.2.6 CDKN2A

CDKN2A, also known as cyclin-dependent kinase Inhibitor 2A is a gene which in humans is located at chromosome 9, band p21.3 [57] and codes for two proteins including *INK4* family member *p16* (or *p16INK4a*) and *p14arf*. [58-59] Both regulate cell cycle, acting as tumor suppressors. *p16* inhibits cyclin dependent kinases 4 and 6, activating the retinoblastoma family of proteins and blocking the progression from G1 to S-phase.[58-59]

CDKN2A somatic mutations are common in the majority of human cancers, with estimates that *CDKN2A* is the second most commonly inactivated gene in cancer after *p53*, including gliomas.[56,57] Studies have confirmed the relationship between

homozygous deletion of *CDKN2A* and malignant tumor progression, suggesting this marker relates with worst prognosis in anaplastic OLG.[38-58]

In a study in 189 samples of patients under the age of 50, with confirmed glioblastoma, Korshunov et al. detected that chromosome 9p21 deletion is related to an unfavourable prognosis.[9]

2. Objectives

Considering that DG are histomorphologically very heterogeneous and harbour different variable prognosis, it is important to stratify patients for their risk level of recurrence. To achieve this goal, we hypothesize that histomorphological and molecular analysis could allow us to conclude relevant prognostic significance. The study aimed to:

- Compare IHC profile and cytogenetic changes from two different surgeries from the same patient, treated for recurrences;
- Identify marker based subpopulations in tumour sample from both surgeries.

3. Ethical Considerations

The study is based on the analysis of human samples, from archives, using formalin fixed paraffin embedded samples, previously used to obtain a diagnosis.

The patients' confidentiality was maintained as samples were identified with letters (A to AF) and only the following variables were considered for the study: age, gender and location of the tumor.

A digital log book was created, identifying only cases and variables and never the personal data of the patients.

The project was presented for approval to the Ethics Committee of the Centro Académico de Medicina de Lisboa, and approved with the reference: 442/16.

4. Material and Methods

4.1 Sampling Method

Cases were selected from the Laboratory of Neuropathology (LN) database. Sampling was achieved using diagnosis as criteria for classification, preserving patients' confidentiality and limiting the access to personal data.

The study aimed to evaluate samples from patients with low grade anaplasia DG, who relapsed with a higher grade tumor. The selection was based on the following criteria (Figure 4):

1. Diagnosis of diffuse glioma;
2. Diffuse gliomas cases whose patients were submitted to two or more surgical resections;
3. Only samples with enough biological material to be used and still remain on archive for any eventual neuropathological techniques.

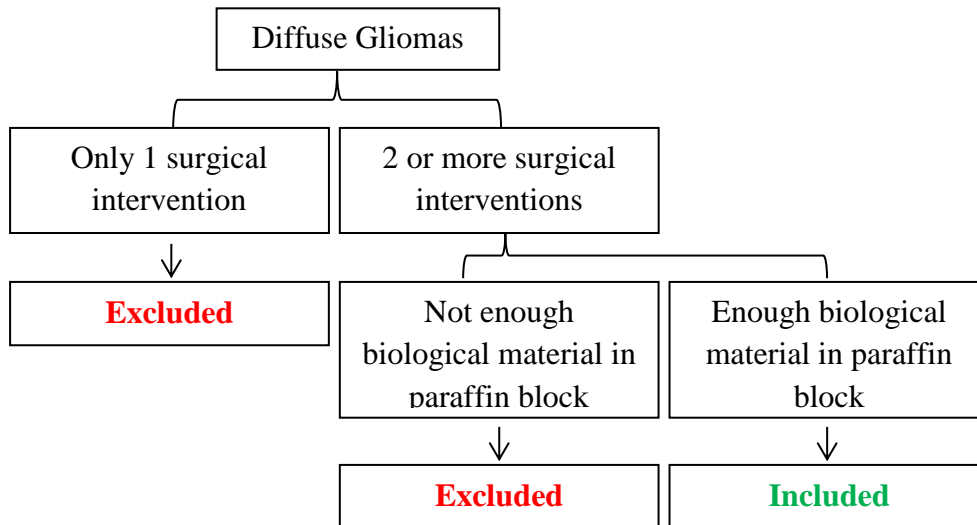


Figure 4- Sampling criteria

Sixteen patients were selected, representing 32 paraffin blocks. From cases with more than one block, only one from each surgery was selected, based on major tumor representativity.

From each block, 5 slides with 2 μ m sections were obtained using a Minot microtome (Leica RM2145), for IHC techniques, in the following order: *GFAP*, *IDH1*, *KI-67*, *ATRX* and *Olig-2*.

Then, Tissue Micro Array (TMA) was performed with 30 of the 32 paraffin blocks, to obtain 2 new TMA blocks with samples from each case, for FISH technique. The punched areas were selected, based on the IHC analysis that revealed major tumor areas of interest. The remaining 2 blocks, that didn't go through TMA, were analysed in their totality due to its limited amount of sample. Sections from these blocks (two TMA and two original) were obtained at 5µm, for the following probes: *CDKN2A*, *EGFR*, *PTEN*, *p53*, *1p* and *19q*.

4.2 Immunohistochemistry

Sections were dewaxed and rehydrated through decreasing alcohol concentrations to water. Endogenous peroxidase was blocked using a 3% hydrogen peroxide solution for ten minutes. Microwave antigen retrieval was performed for ten minutes at 600W followed by twenty minutes at 850W, using H3300 vector citrate buffer. Slides were rinsed in phosphate buffered saline (PBS) and incubated with the respective primary antibody, overnight (ON) at 4°C.

Sections were then rinsed twice in PBS and incubated with secondary antibody, Dako REAL™ Envision™ HRP Rabbit/Mouse, for 1 hour at room temperature (RT). Slides were rinsed in PBS, stained with 3,3'-diaminobenzidine (DAB) solution for five minutes and rinsed in tap water. Counterstain was provided by Harris Hematoxylin for 4 minutes, and then slides were then differentiated, blued with 1% ammoniacal water, dehydrated, cleared and mounted with synthetic mounting media, Entellan® (Appendix 1).

4.3 Fluorescent *In Situ* Hybridization

As in the previous procedure, slides with the sections were dewaxed and rehydrated through decreasing alcohol concentrations to water. Microwave antigen retrieval was performed for 10 minutes at 600W followed by 20 minutes at 850W, using in H3300 vector citrate buffer. Slides were rinsed, following Vysis Paraffin Pretreatment IV & Post-Hybridization Wash Buffer Kit in a pre-hybridization solution of Sodium thiocyanate, pre-heated in the oven at 82°C, for 10 minutes. After a quick rinse in ethanol, slides were incubated for 10 minutes in Pepsin solution (Vysis Protease IV), at 37°C, rinsed again in ethanol and left to air dry for 10 minutes.

Probes were applied following Abbott Vysis probes protocol (10µL in each slide). The incubation took place in a ThermoBrite Leica System Hybridizer, from Abbott Molecular, twenty minutes at 72°C followed by overnight at 37°C.

The next day, slides were put in two post-hybridization solutions, first for about 10 minutes, until the coverslips fell down, and second one, pre-heated at 75°C, for 2 to 3 seconds.

Slides were rinsed in distilled water, stained with DAPI solution for one minute at RT, rinsed in tap water, dehydrated, cleared and mounted synthetic with mounting media, Entellan® (Appendix 2).

4.4 Data Analysis

4.4.1 *ATRX*, *IDH1* and *GFAP*

IHC slides were observed in bright-field microscope for staining quality control and photographed using Canon EOS 1200D camera, with a EF-S 18-55mm lens in auto mode. Images were saved in .tiff format and analysed in Image-J [59], using the colour deconvolution plugin.[60] Areas of interest – black – were measured and colours were assigned to black images, one for each antibody (Figures 5 and 6). Superimposition was made and those areas – primary colours – were measured.

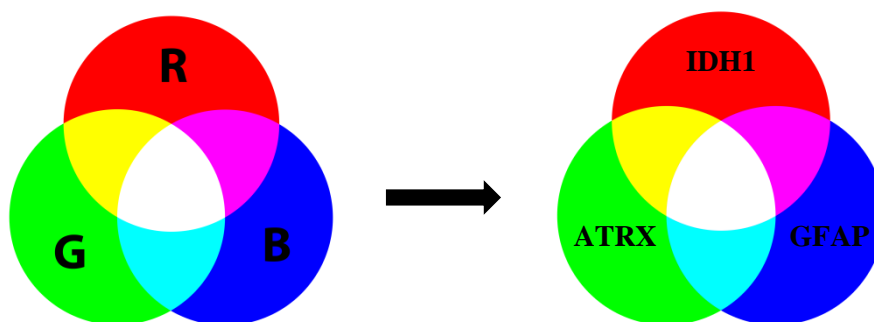


Figure 5 - RGB and primary colour scheme used in Image-J analysis

Primary colours areas represented subpopulations of tumor cells that expressed two proteins at the same time. Data was treated in pixels and final results were converted to percentages for easier understanding.

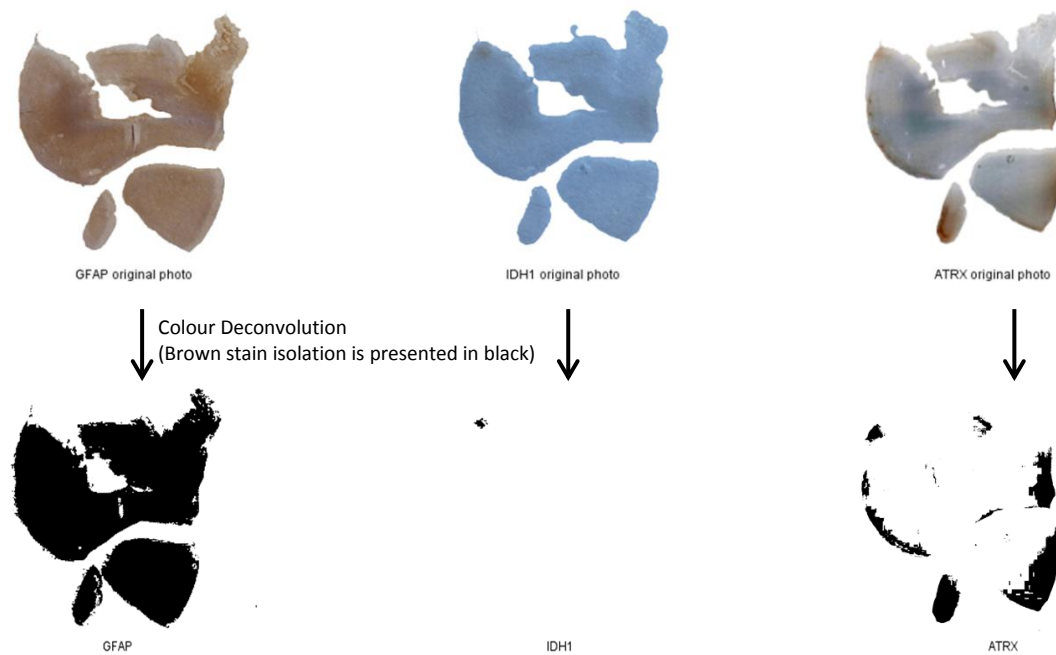


Figure 6 - On top: Photographs from the IHC slides of one of the cases. Bellow: The isolation of the brown areas (expression of antibodies), converted in black. (From left to right: GFAP, IDH1 and ATRX)

Original photographs were converted into black and white images, where the background was white and the brown marked areas were converted to black (Figure 6). Black and white images were then turned into RGB ones, where background colour was inverted to black and the marked areas were assigned with primary colours. Images were then overlapped and the colours added, resulting in a final image, where it was possible to visualize colocalization areas of both markers (Figure 7 and Table 1).

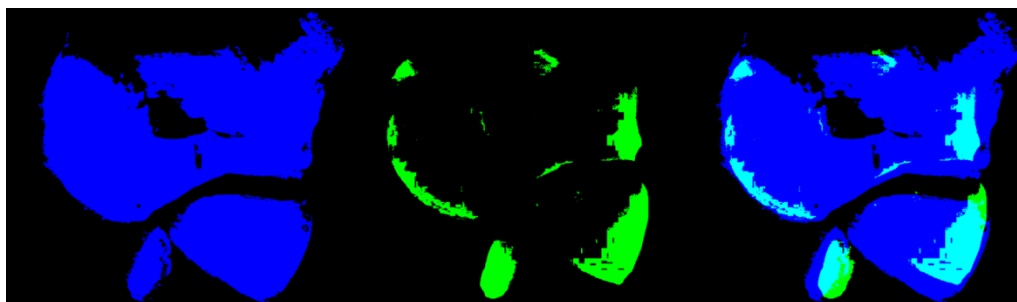


Figure 7 - Overlap of two different antibodies (*GFAP* and *ATR*) through the attribution of primary s to the stained areas. (*GFAP* - blue; *ATR* - Green; Overlap - Cyan)

Table 1 - Image-J table of coloured Areas.

Results					
	Color	Color Pixels	Total Pixels	Particles	% Color
1	Green	68409	909675	325757.143	7.520
2	Blue	421967	909675	2009366.667	46.387
3	Cyan	60672	909675	288914.286	6.670

The obtained table with the areas for each colour helped to identify the subpopulation we were looking for, namely: *GFAP+ATRX+*.

4.4.2 *Olig-2* and *KI-67*

Afterwards, areas of the tumor slides immunostained by *Olig-2* and *KI-67* were selected to be photographed. Three photographs per slide were obtained in bright-field microscope Leica DM 4000 B, using an amplification of 400x, and the ratio stained/non-stained cells was obtained in Image-J (Figure 8), with the plugin ImmunoRatio. [61]

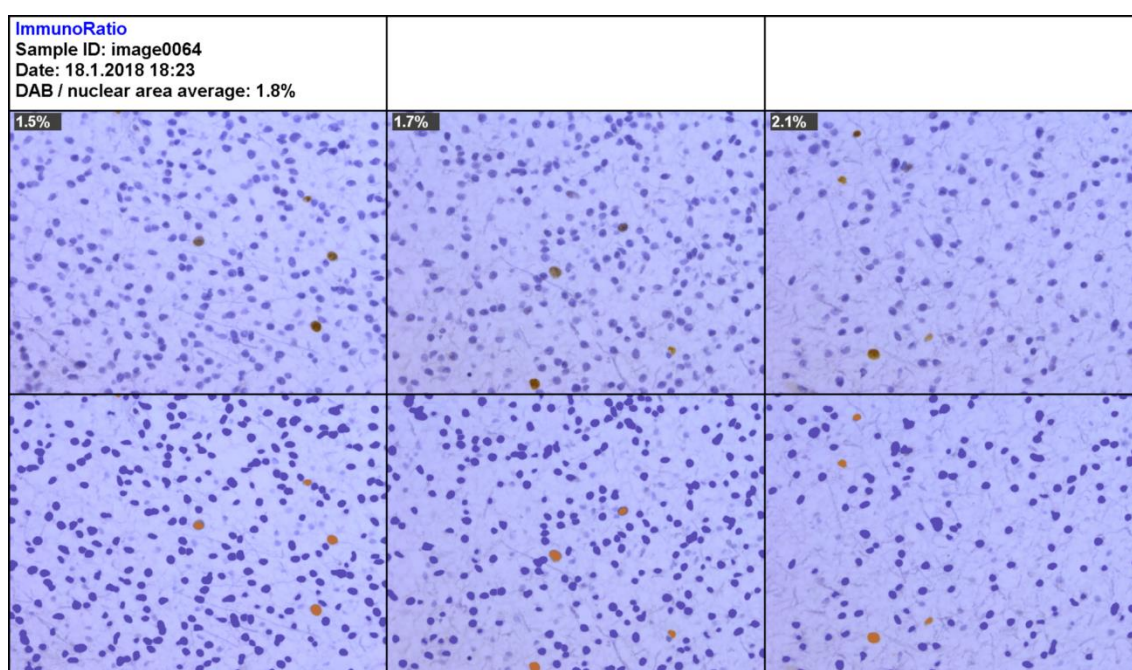


Figure 8 - Example of the application of the plugin ImmunoRatio in a sample slide stained for *KI-67*. Three distinct fields where photographed and the ratio between stained nuclei and non-stained nuclei were obtained. On top are the original photographs and at the bottom are the nuclei considered to the calculation.

4.4.3 FISH

FISH slides were photographed in Fluorescence Microscope Leica DM 4000 B, using appropriate filters. Cells with amplification or deletion of the studied genes were counted (Table 2), using the plugin Cell Counter [62] on Image-J.

Table 2 - Type of mutation by gene

Gene	Deletion	Amplification	Other Specifications
<i>1p</i>	✓		
<i>19q</i>	✓		
<i>CDKN2A</i>	✓		
<i>PTEN</i>	✓		
<i>P53</i>	✓		
<i>EGFR</i>		✓	Simple Gene Amplification or Clusters

4.4.4 Statistics

Descriptive statistical analysis was performed. Numerical results from all cases were analysed using absolute values, and calculating mean and standard deviation for comparing purposes. Graphics were obtained using SigmaPlot 12.0, and tables were obtained using Excel and Image-J.

5. Results

The study included 18 OLG, 3 OLGA, 10 AT and 1 Gliosarcoma (GS) (Table 3).

Table 3- Proportion of samples in the study divided by histological classification

	# Samples	Percentage of total (%)
Oligodendroglioma	18	56,250
Oligoastrocytoma	3	9,375
Astrocytoma	10	31,250
Gliosarcoma	1	3,125
Total	32	100,000

Five antibodies were studied in each sample, resulting in a total of 160 IHC slides.

- From primary to relapse tumors, the expression of *KI-67* is generally higher in relapses (Figure 9). The maximum percentage of expression for *KI-67* was 17,1%, in a relapse sample (Figure 10). The opposite is observed in *Olig-2*, where primary samples presented higher values compared to relapses (Figure 11 and 12).

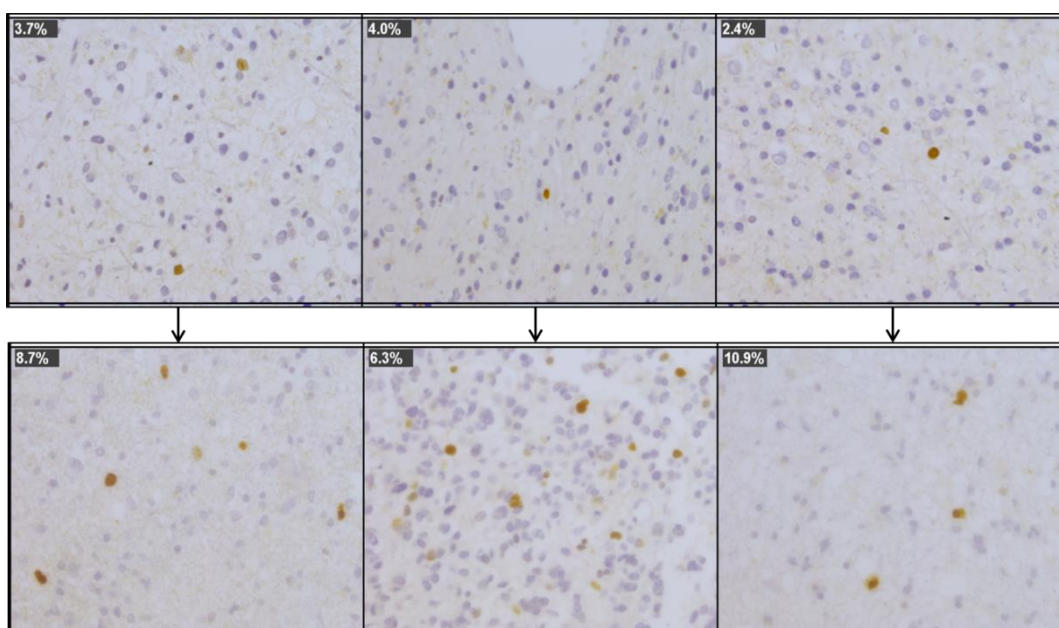


Figure 9 - Example of the evolution of *KI-67* from primary tumor sample (top images) to relapse tumor sample (bottom images). Three fields of each slide were photographed and the DAB/Nuclear area average ratios found were: Primary tumor sample – 3,4% and Relapse tumor sample – 8,6%.

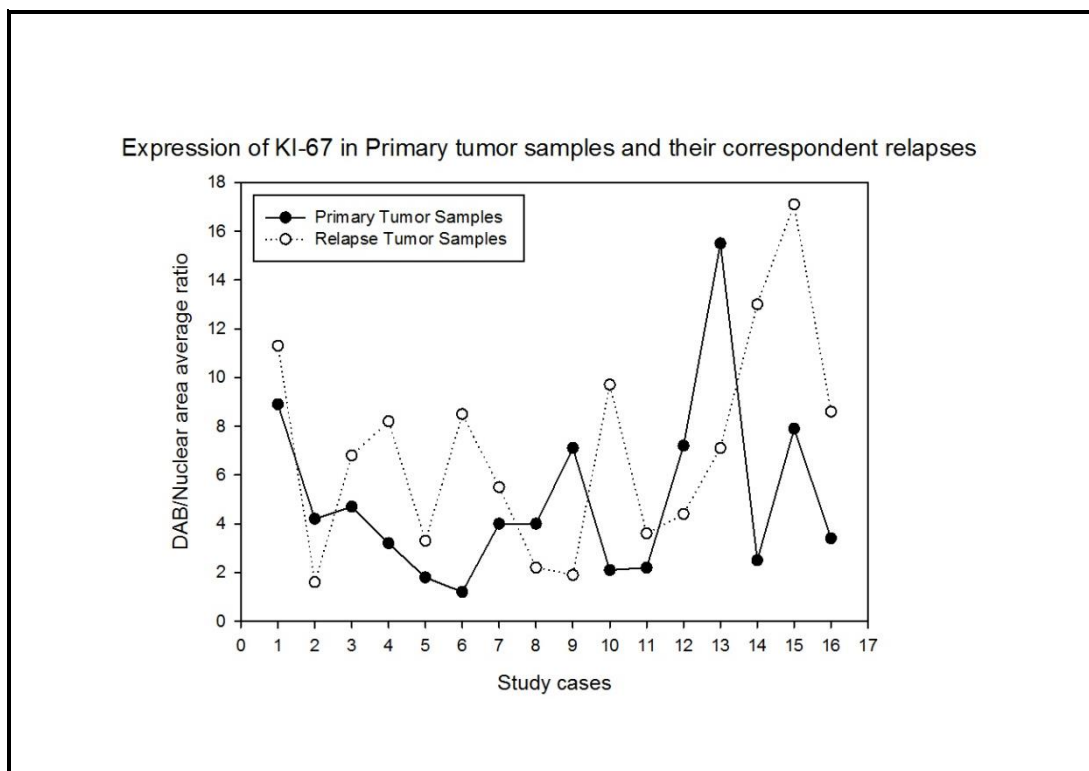


Figure 10 - Evolution of the expression of individual markers from primary tumors to their relapses.

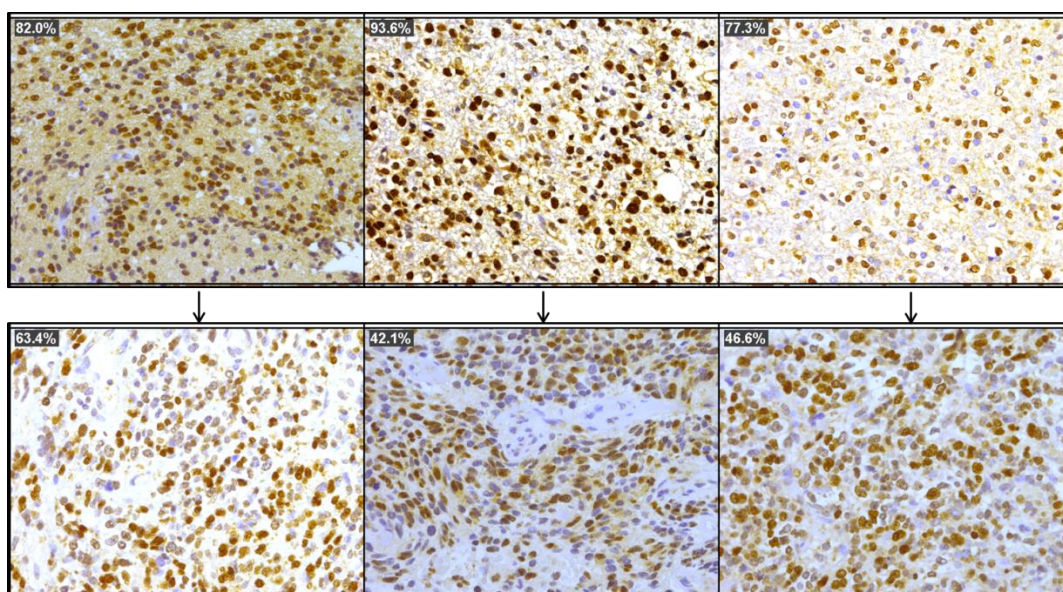


Figure 11 - Example of the evolution of *Olig-2* from primary tumor sample (top images) to relapse tumor sample (bottom images). Three fields of each slide were photographed and the DAB/Nuclear area average ratios found were: Primary tumor sample – 84,3% and Relapse tumor sample – 50,7%.

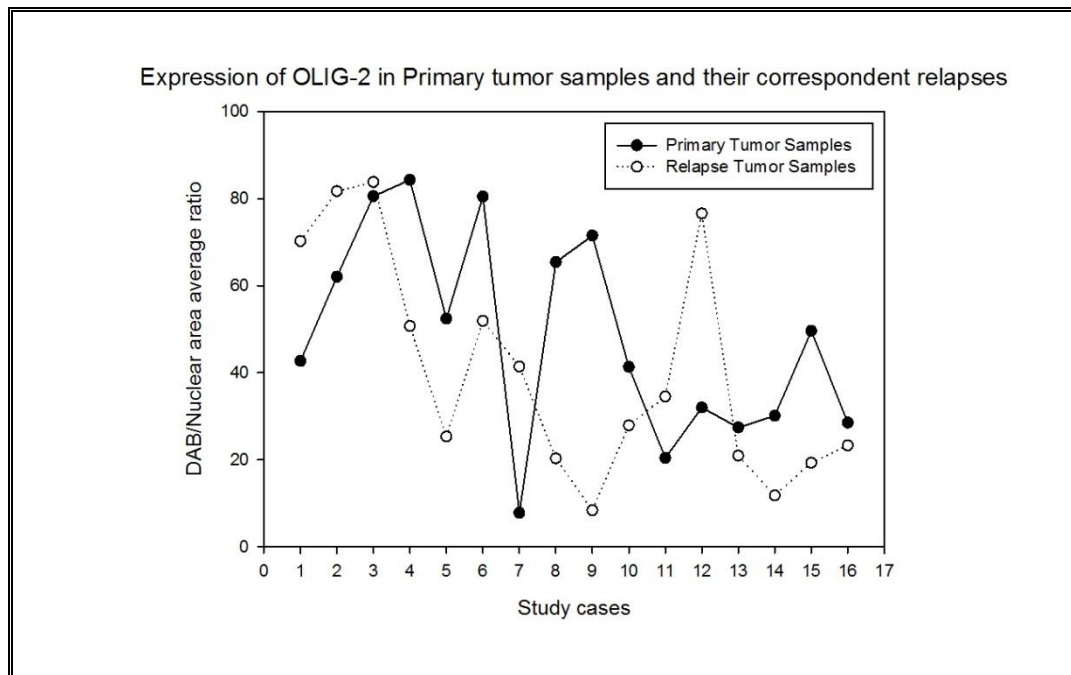


Figure 12 - Evolution of the expression of individual markers from primary tumors to their relapses.

- *IDH1* areas showed a reduction or no changes in most cases and *ATRX* areas were reduced and increased in the same proportion (Figure 13). Percentage of *IDH1mut* areas found was generally low, varying between 0 and 3,38%.

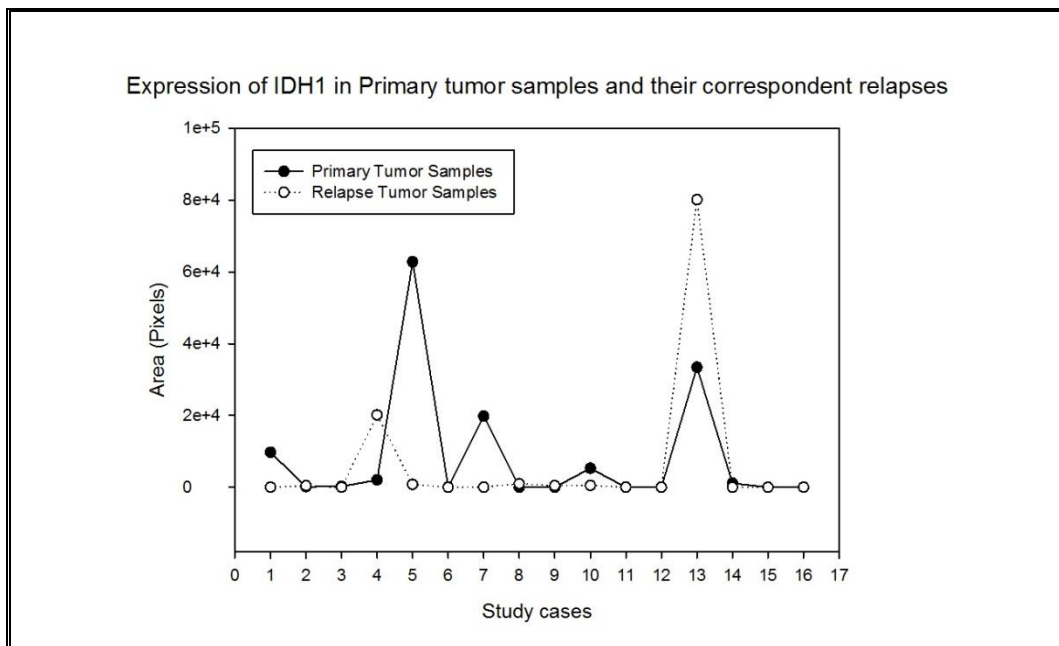


Figure 13 - Evolution of the expression of individual markers from primary tumors to their relapses.

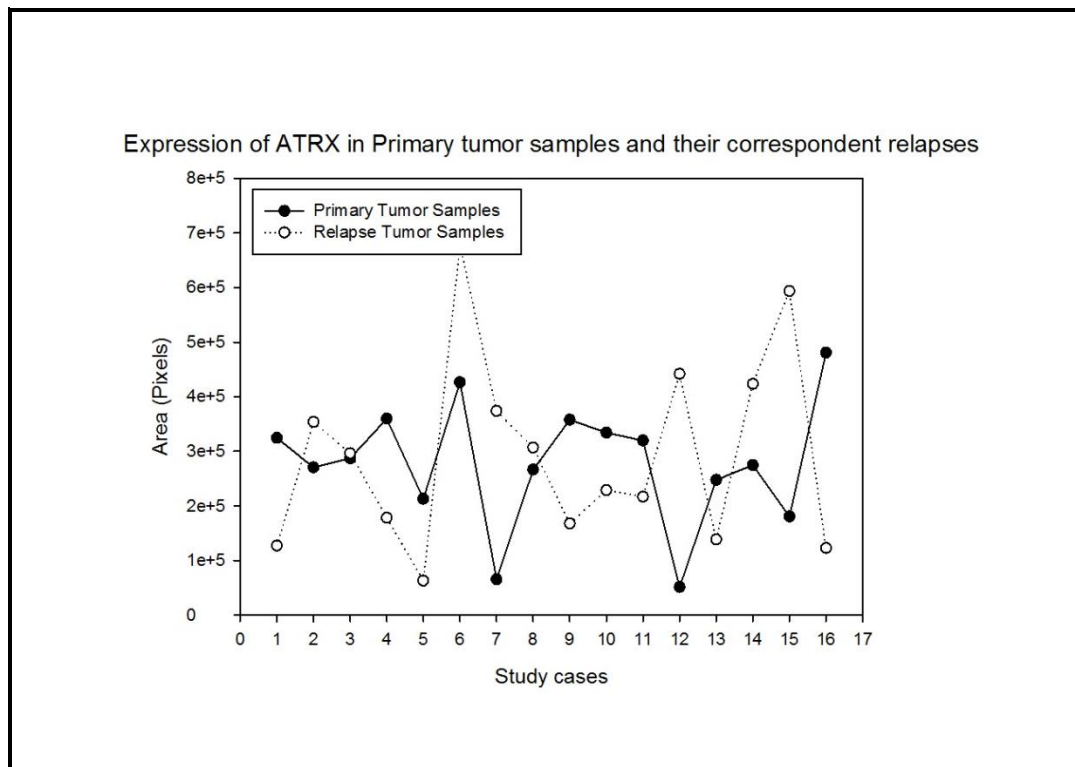


Figure 13 (cont.) - Evolution of the expression of individual markers, from primary tumors to their relapses.

- It was possible to identify tumor cells subpopulations with different protein expression combinations. As mentioned above, this analysis was based on the study of different layers of the same tumor samples and the following comparison between the subpopulations found in primary and relapse tumors (Figure 14).

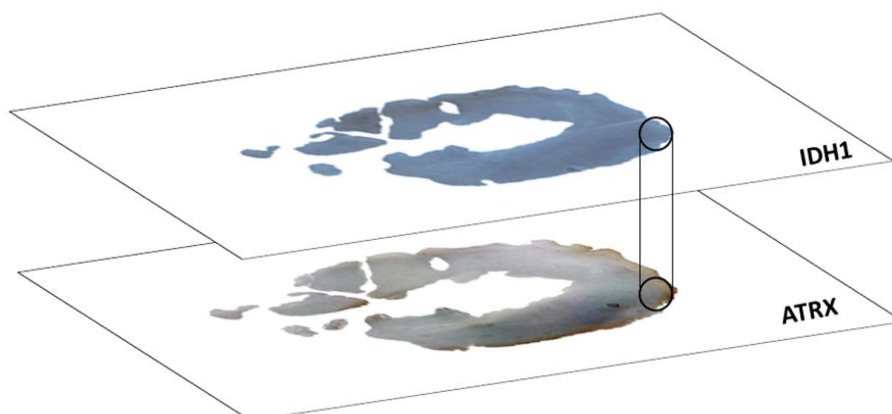


Figure 14- Illustration of the layered analysis performed in the samples showing the colocalization spots of two antibodies, which represent subpopulations of cells with different protein expressions.

- When searching for subpopulations of tumor cells, the following ones were studied, initially:

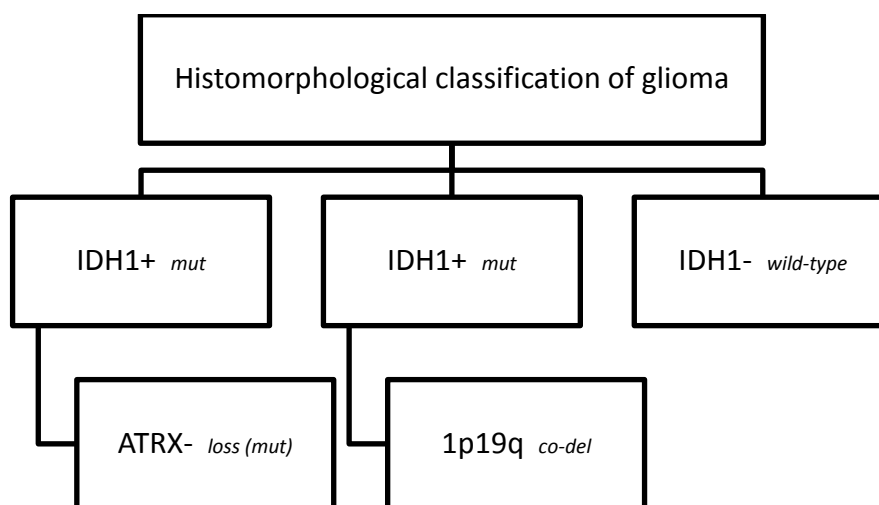


Figure 15- Tumor Subpopulations of cells studied.

The above subpopulations (Figure 15) were obtained using the following formulas:

Table 4 – Formulas used for the calculation of areas

Subpopulation	Used formula	Explanation
<i>IDH1+ATRX-</i>	$A = R$	Area obtained equals area of red.
<i>IDH1+1p19qco-del</i>	$A = (R + Y) \cap co-del$	Area obtained is the result of red plus yellow areas and the intersection of that value with <i>1p19q</i> co-deleted areas.
<i>IDH1-</i>	$A = \bar{R} \Leftrightarrow B - R$	Area obtained equals area of non-red, which means is the subtraction of red from blue (total).
<p><i>Note:</i></p> <ul style="list-style-type: none"> ▪ <i>IDH1+</i> = mutation (detected by IHC) ▪ <i>IDH1-</i> = WT protein (undetected by IHC) ▪ <i>ATRX+</i> = presence of protein (detected by IHC) ▪ <i>ATRX-</i> = loss of protein (undetected by IHC) 		

- As showed in Figure 16, *IDH1mut/ATRXloss* area presents very close values in both groups – primaries and relapses, being mean and standard deviation 5053 ± 10116 from primaries and from relapses. Linearized ratio between these two groups obtained by Pearson's correlation coefficient is $p=0,852$ with relapses tumor samples presenting a bigger area expressing *IDH1mut/ATRXloss* cells.

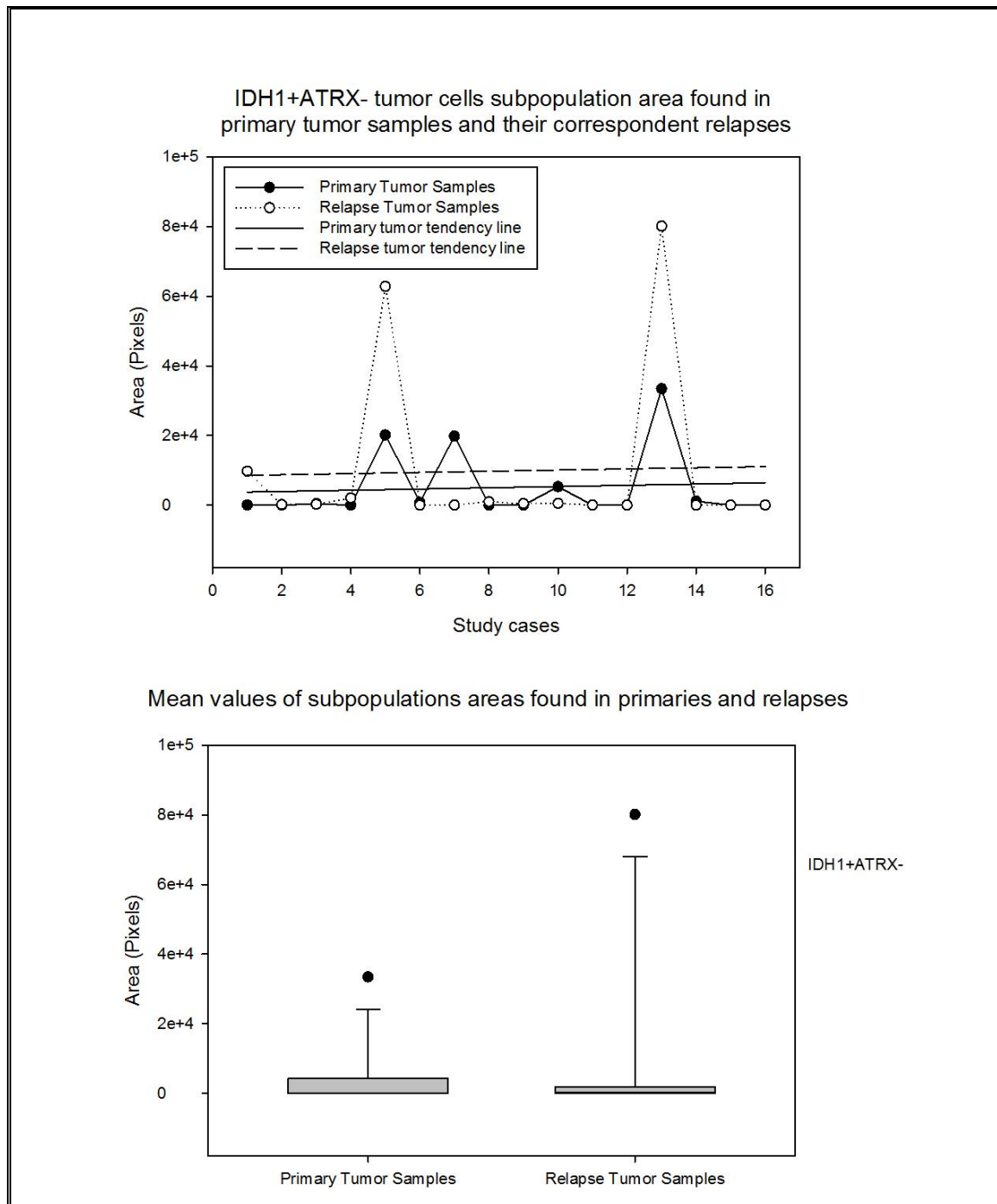


Figure 16 – Comparison of mean values of subpopulations of tumor cells from primary tumors to their relapses.

- Regarding *IDH1*_{wt} cells, values are inverted with a p-value of -0,432, where primary tumors group mean and standard deviation is 671939±180448 and the relapses group is 609653±284091 (Figure 17).

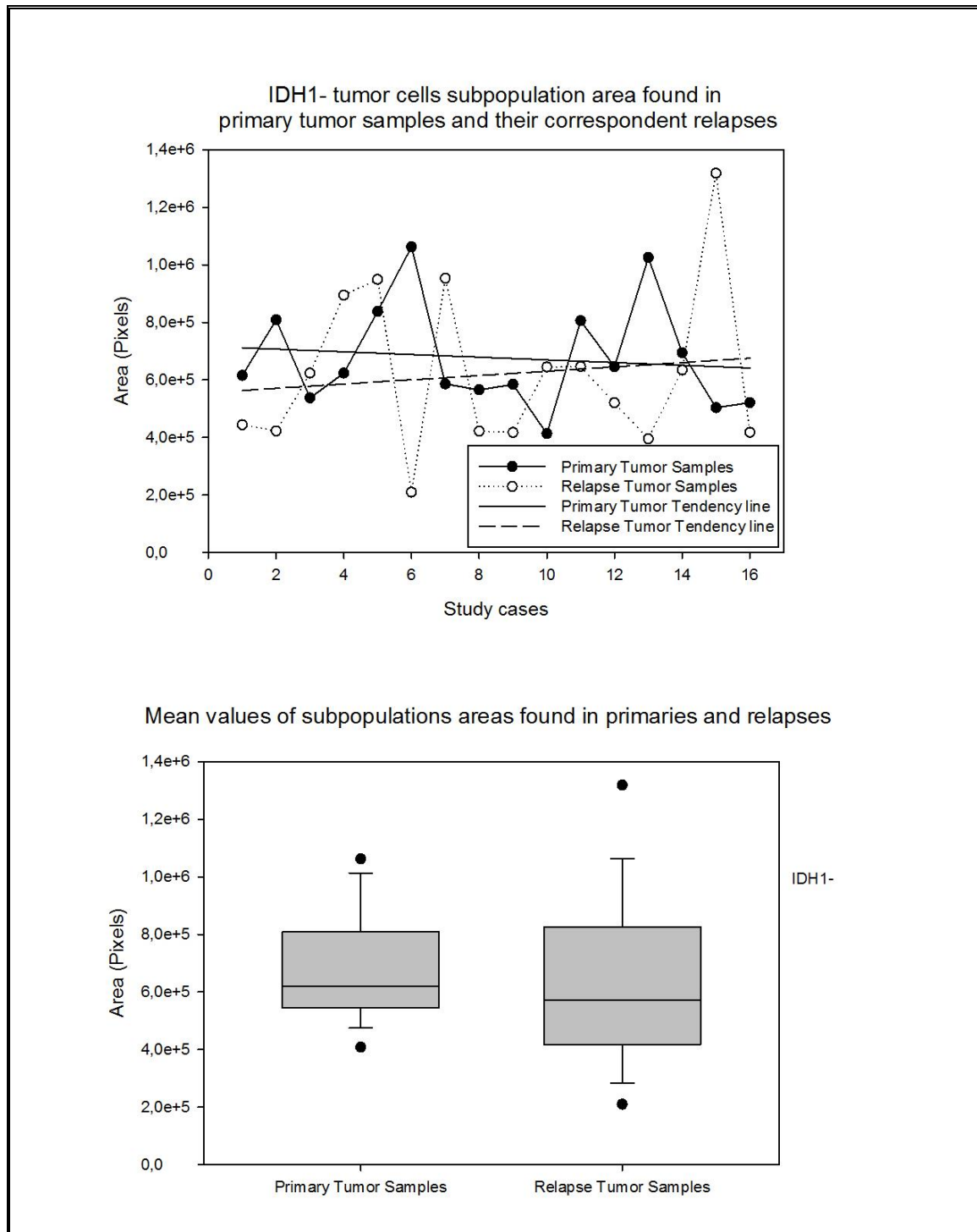


Figure 17 - Comparison of mean values of subpopulations of tumor cells from primary tumors to their relapses.

Table 5 shows the relation between *IDH1mut/ATRX* subpopulations and *1p19q* co-deletion.

Table 5 - *IDH1mut/ATRX/1p19q* co-deleted subpopulations

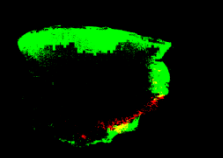
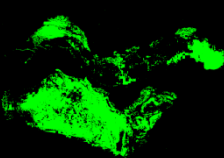
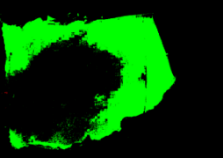
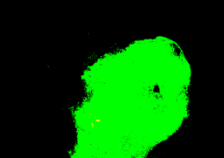
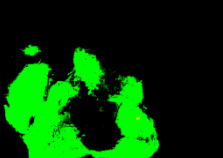
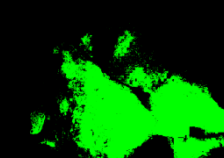
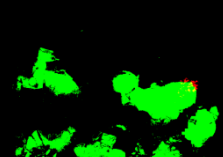
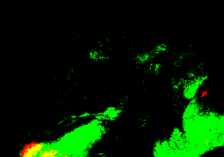
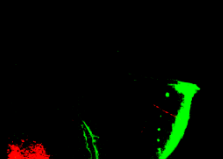
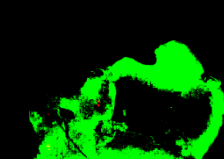

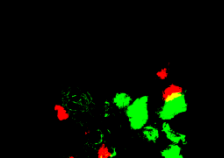

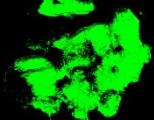

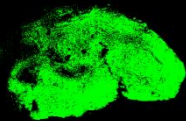
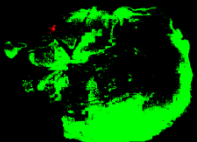
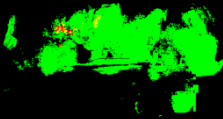
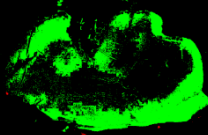

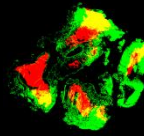
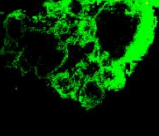
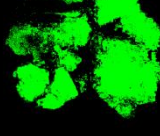
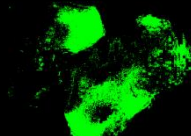
Case	Primary Tumor				Relapse Tumor			
	Image	% <i>IDH1</i> +/ <i>ATRX</i> +	% <i>1p</i> deleted	% <i>19q</i> deleted	Image	% <i>IDH1</i> +/ <i>ATRX</i> +	% <i>1p</i> deleted	% <i>19q</i> deleted
1		0,00	34,31	22,40		0,86	45,45	20,29
2		0,00	36,07	28,97		0,00	14,42	17,79
3		0,07	13,75	2,26		0,04	9,56	3,76
4		0,00	6,03	6,90		0,11	17,09	9,09
5		1,96	8,59	12,16		0,89	6,56	7,94
6		0,03	8,77	8,19		0,00	9,33	5,07

Table 5 (cont.) - *IDH1mut/ATRX/1p19q* co-deleted subpopulations

Case	Primary Tumor				Relapse Tumor			
	Image	% <i>IDH1</i> +/ <i>ATRX</i> +	% <i>1p</i> deleted	% <i>19q</i> deleted	Image	% <i>IDH1</i> +/ <i>ATRX</i> +	% <i>1p</i> deleted	% <i>19q</i> deleted
7		0,44	33,90	4,85		0,00	7,80	1,24
8		0,00	10,37	24,53		0,11	11,36	26,04
9		0,00	9,35	16,24		0,00	18,67	30,33
10		0,87	9,57	62,96		0,00	3,54	28,48
13		0,00	0,00	11,43		9,44	18,64	7,14
14		0,14	1,89	10,00		0,00	3,82	11,36

- Of all *IDH1mut/ATRX* primary tumors, only about 33% maintained this expression in relapses. Regarding primary tumors without *IDH1mut/ATRX* expression, 40% started to express both these markers in relapses. *IDH1mut/ATRX/1p/19q* co-deleted cells were found in only 1 out of 16 cases.

- 1p gene was found deleted in only 4 samples, being 3 OLG (two low-grade) and 1 AT (low-grade).

19q gene was found deleted in 5 samples, being 3 OLG (one low-grade) and 2 AT (1 low-grade and 1 higher-grade).

Co-deletion of *1p/19q* was only found in 1 case of low-grade OLG which relapsed in a higher-grade OLG with no deletions of these genes.

Although it was not the focus of the study, comparison between diagnostic groups was performed, for subpopulations. Histological classifications were assigned according to WHO parameters approved prior to the 2016 review.

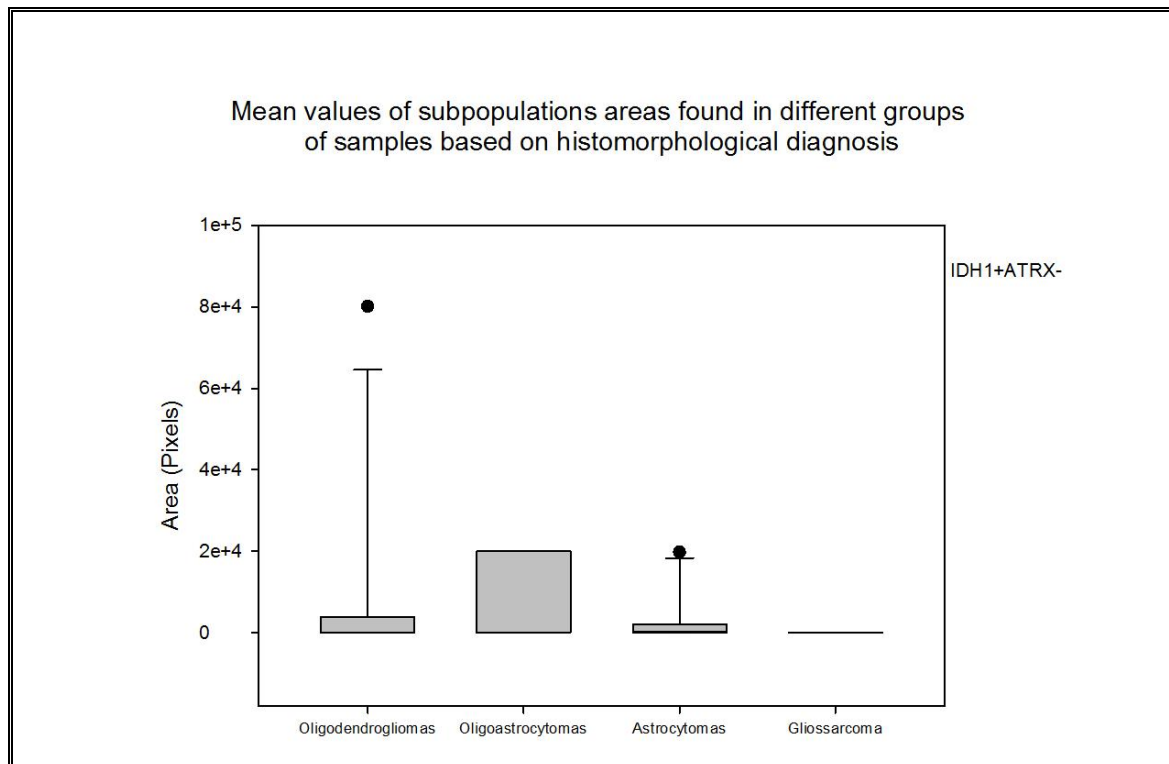


Figure 18- Comparison of mean values of subpopulations of tumor cells among different groups based in histomorphological diagnosis.

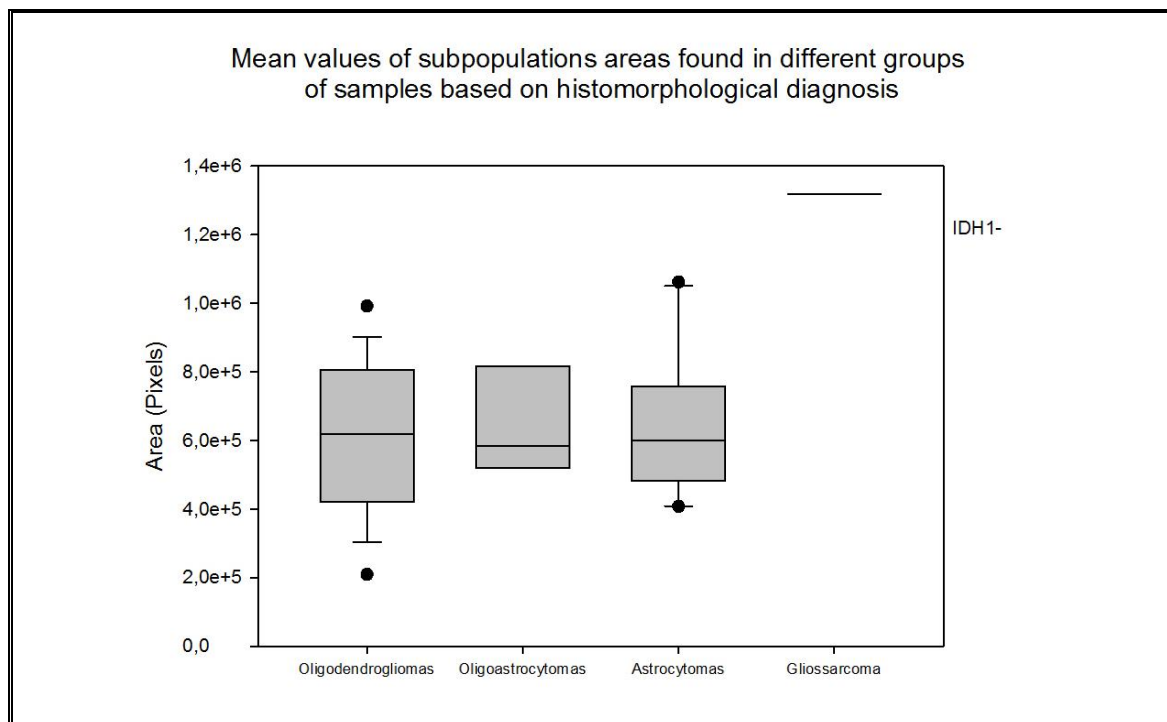


Figure 18 (cont.) - Comparison of mean values of subpopulations of tumor cells among different groups based in histomorphological diagnosis.

- Figure 18 shows *IDH1*mut/*ATRX*loss area means values and respective standard deviations decreases in the following order OLG (10562,72±23719,45), OLGA (6708,33±11619,17), AT (2738,40±6199,81), and GS (0).
- Regarding *IDH1*wt cells, values vary in almost the same order of categories, decreasing from GS (1318048) to OLGA (640779,7±156722,6), to AT (640361,2±216242,5), to OLG (603415,7±213690,4).
- We found 57% of primary tumors with *IDH1* mutation kept it in their correspondent relapses. (Figure 19). From primary tumors without this mutation, about 56% developed it in relapses (Figure 19).

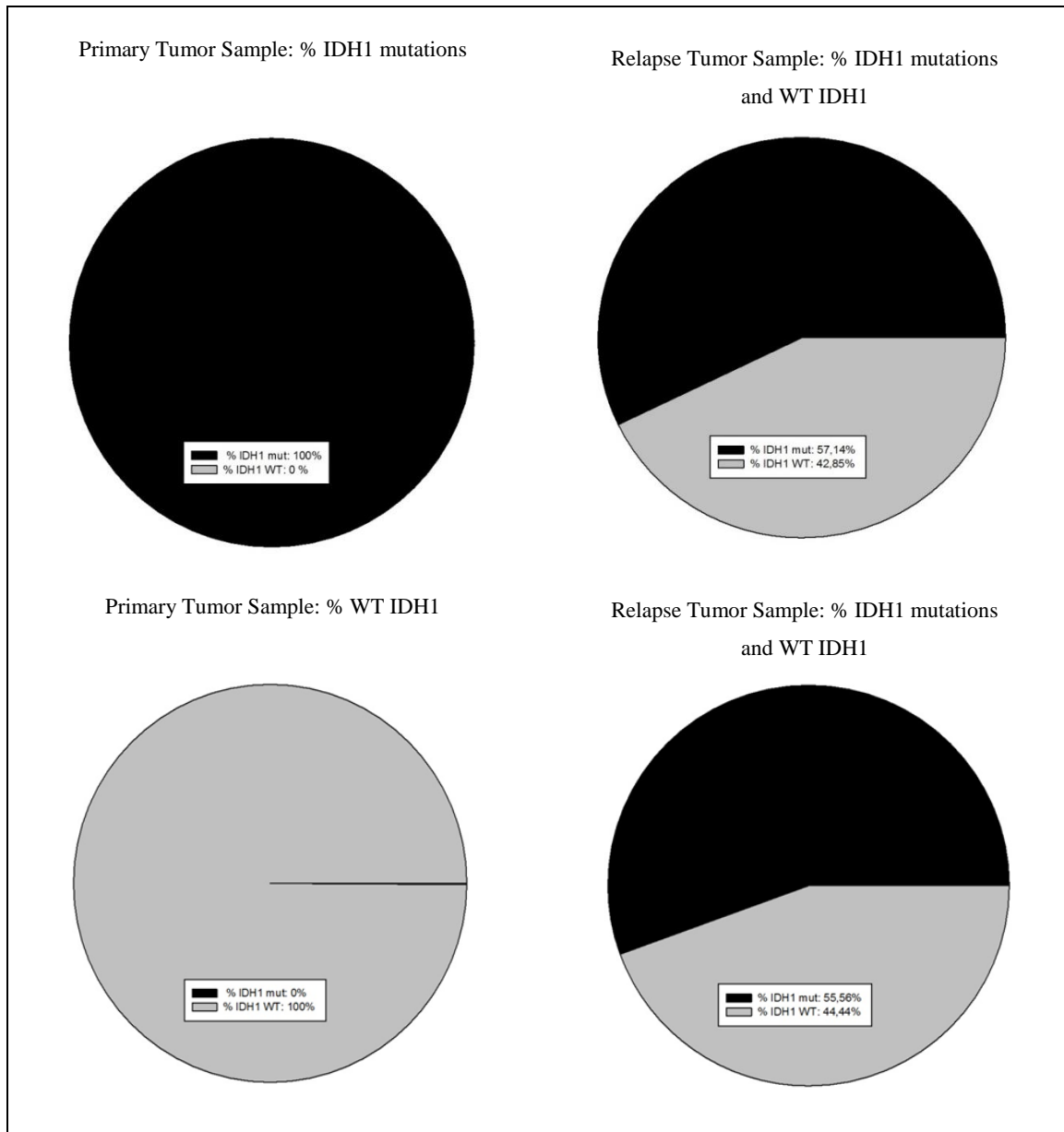


Figure 19 - *IDH1* mutation profiles in primary and relapse tumors.

- FISH analysis of the other probes, showed the percentage of nuclei with deletion of tumor suppressor gene *PTEN* was low in all samples, ranging from 1,78% to 14,29%. [63]
- *EGFR* study showed amplification in 6 of 32, of which four correspond to AT (1 primary and 3 relapses, most of them with multiple copies of the gene and only 1 with clusters), and 2 correspond to OLG, both in relapses with more than 4 copies (Table 6).

Table 6 - *EGFR* FISH positive results.

Sample	Tumor	Diagnosis	<i>EGFR</i>		
			% clusters	% 4 copies	% > 4 copies
12	Relapse	Oligodendroglioma	4,65	9,30	13,95
13	Primary	Astrocytoma	6,06	9,09	15,15
14	Relapse	Astrocytoma	4,00	9,71	13,71
16	Relapse	Oligodendroglioma	5,43	5,43	10,85
20	Relapse	Astrocytoma	13,04	0,00	13,04
28	Relapse	Astrocytoma	7,30	13,87	21,17

Comparing the differences from primary tumors to their relapses (Figure 20), in 4 cases *EGFR* was not amplified in the primary and became amplified in some form in the relapse, namely 1 astrocytoma which relapsed as an OLG (*EGFR* variation from 0 clusters + 5,71% 4 copies + 5,71% > 4 copies to 4,65% clusters + 9,30% 4 copies + **13,95% > 4 copies**); 1 primary OLG (6,52% 4 copies + 6,52% > 4 copies) which relapsed as a higher-grade OLG (5,43% clusters + 5,43% 4 copies + **10,85% > 4 copies**); 1 low-grade AT (4,76% clusters + 4,76% 4 copies + 9,52% > 4 copies) which relapsed as a higher-grade AT (**13,04% clusters + 13,04% > 4 copies**) and 1 AT with no amplification of any kind in the primary which relapsed as a higher-grade AT with 7,30% clusters + **13,87% 4 copies + 21,17% > 4 copies**.

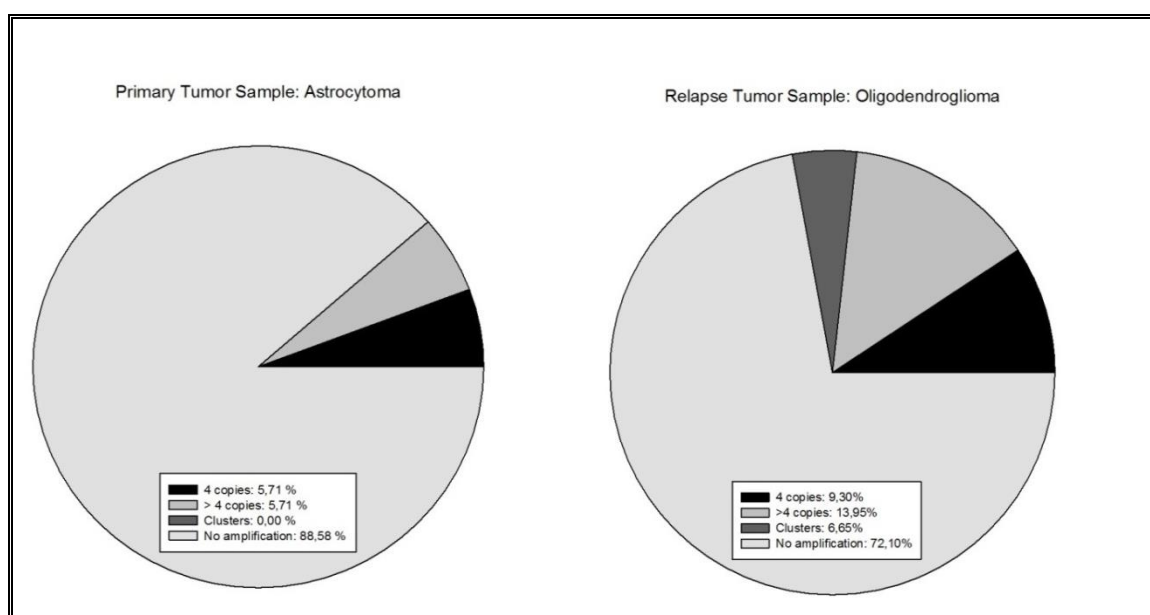


Figure 19- Variations found in *EGFR*, increase in amplification from primary tumor samples to relapses.

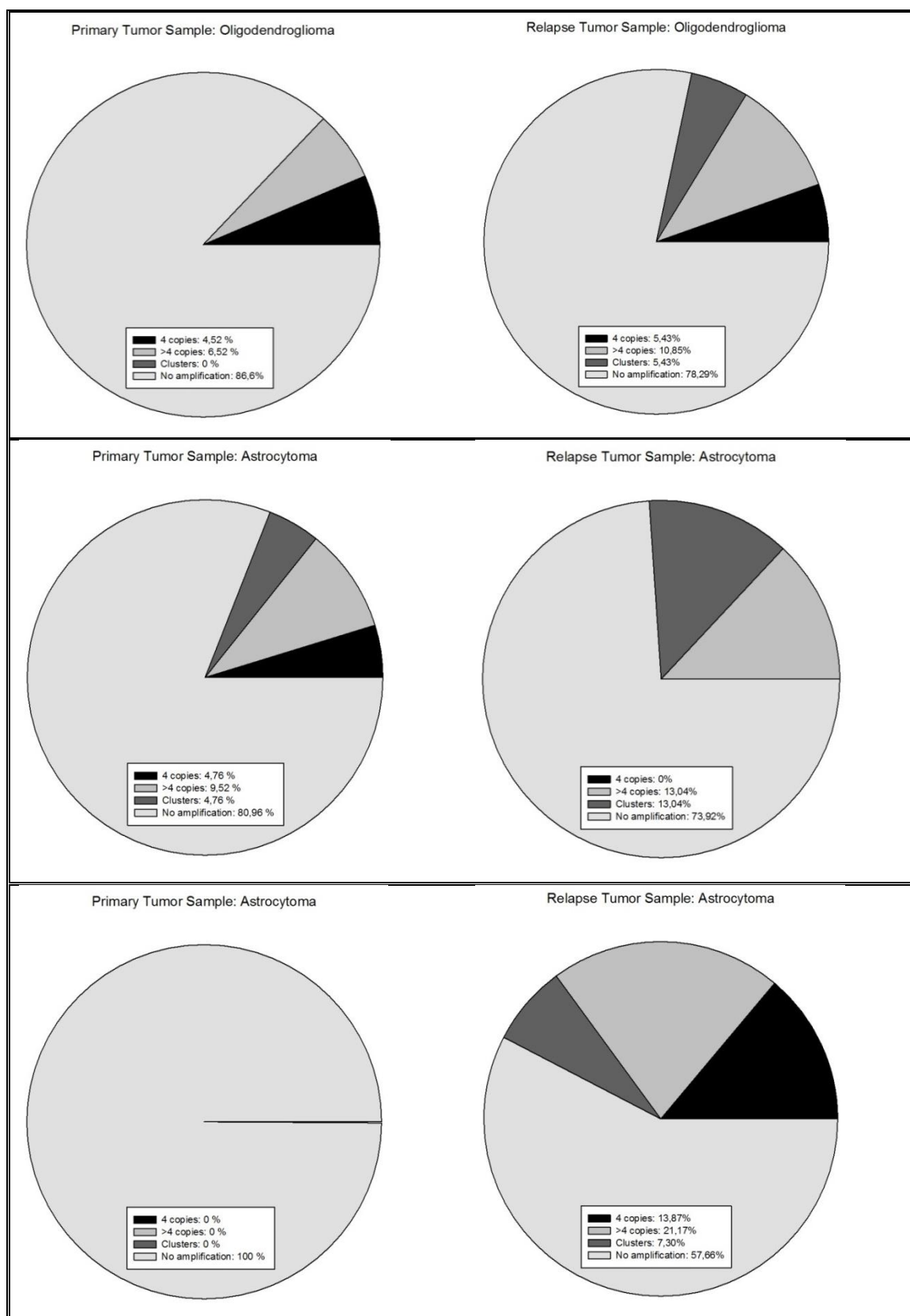


Figure 20 (cont.) - Variations found in *EGFR*, increase in amplification from primary tumor samples to relapses.

One case presented with reduced amplification from primary tumor to relapse (Figure 21 and Appendix 3), namely an AT with 6,06% clusters + 9,09% 4 copies + **15,15% > 4 copies** which relapsed a similar higher-grade with 4,00% clusters + 9,71% 4 copies + **13,71% > 4 copies**. These values seem almost virtually equal and this difference is probably related to the sampling location.

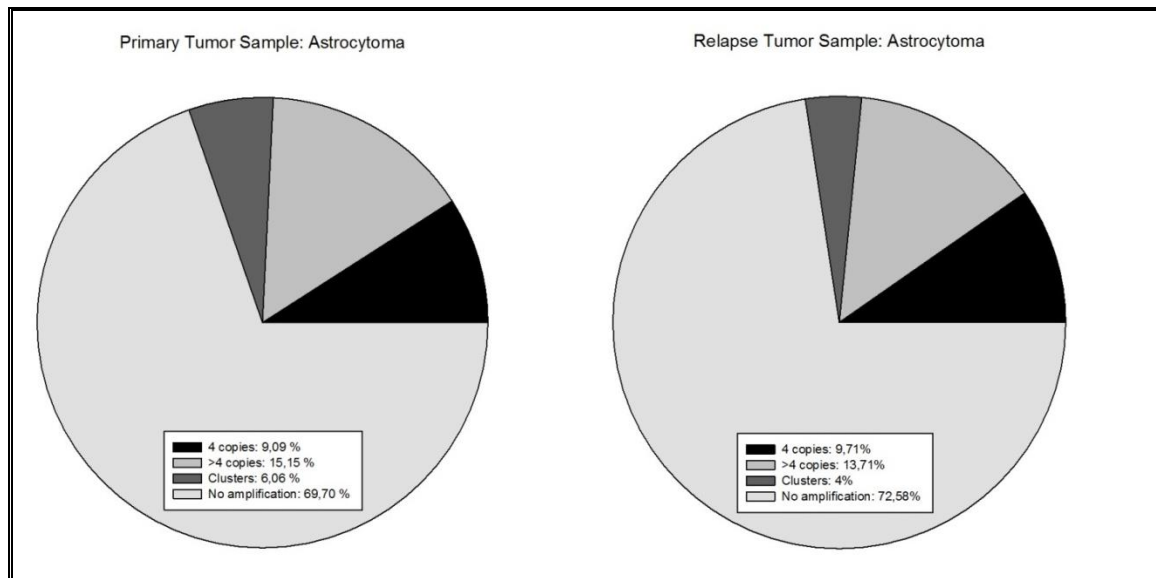


Figure 20 - Variations found in *EGFR*, decrease in amplification from primary tumor samples to relapses.

- *P53* was mutated in 6 samples, being 2 OLG, 2 OLGA and 2 AT. 4 of all 6 mutations occurred in relapses (Table 7). Analysing the changes from primary tumor samples to relapse samples, we found 4 cases with WT p53 in the primary tumors and mutation in relapses and 1 case that kept the mutation in both surgeries.

Table 7 - *p53* mutations.

Sample	Tumor	Diagnosis	% p53 mutation
8	Relapse	Oligodendroglioma	34,21
17	Primary	Oligoastrocytoma	43,88
24	Relapse	Oligoastrocytoma	37,29
26	Relapse	Oligodendroglioma	26,39
31	Primary	Astrocytoma	26,25
32	Relapse	Astrocytoma	32,63

Analysing variations from primary tumors to correspondent relapses (Appendix 4), we found 3 cases (OLG) that had wild-type *p53* gene in primary tumors and mutated form in relapses (Figure 22); 1 OLGA with mutation in the primary tumor which relapsed as OLG without mutation. We also found 1 low-grade AT that kept *p53* mutation in its higher-grade relapse (samples 31 and 32). As shown in the table above, the variation went from 26,25% to 32,63%, raising about 6,38% from primary to relapse.

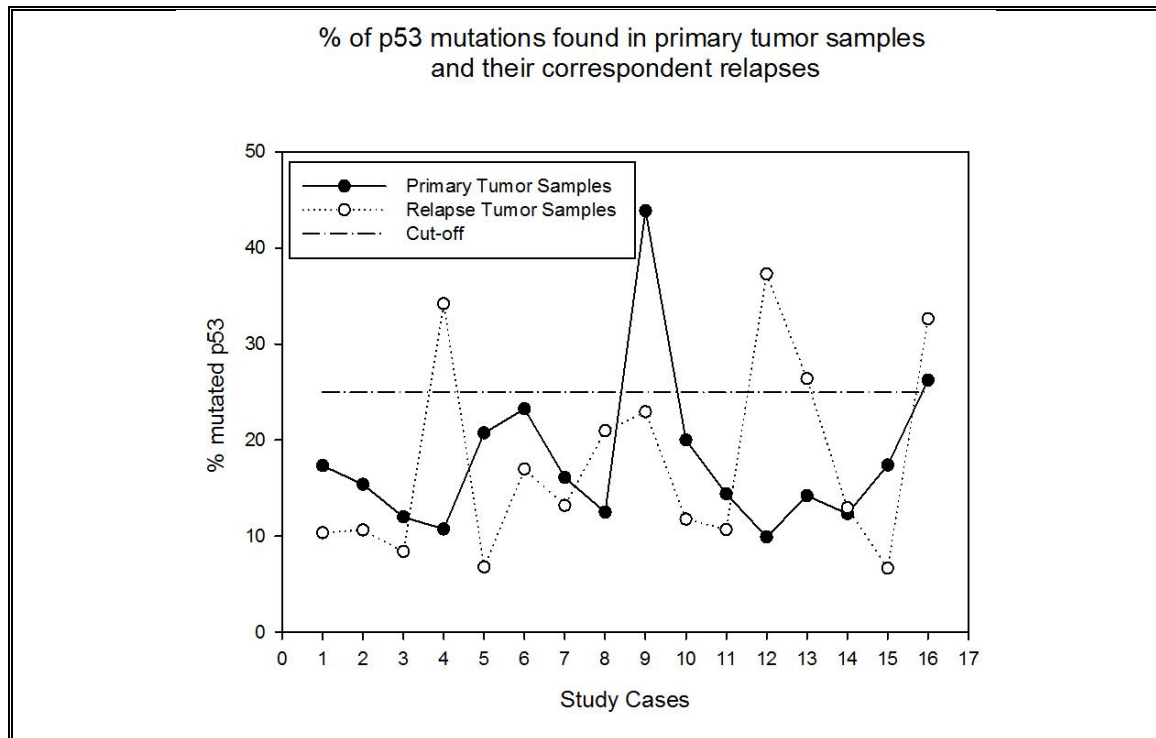


Figure 21 - *p53* mutations found in primary tumor samples and relapses.

- Concerning *CDKN2A* deletions (Figures 23 and 24), we found only 1 case with deletion in both primary tumor and relapse. Results showed 6 cases with deletion in primary tumor and only 3 in the higher-grade relapses. Observing histology-based diagnosis, it is found that *CDKN2A* is deleted in a proportion of ½ of AT to OLG (3 AT and 6 OLG, low-grade or higher-grade). We found the percentages of nuclei with *CDKN2A* deletion ranged from 2,92% to 39,60%, with 9 samples with values over 25%, which can be considered high values (Figure 24).

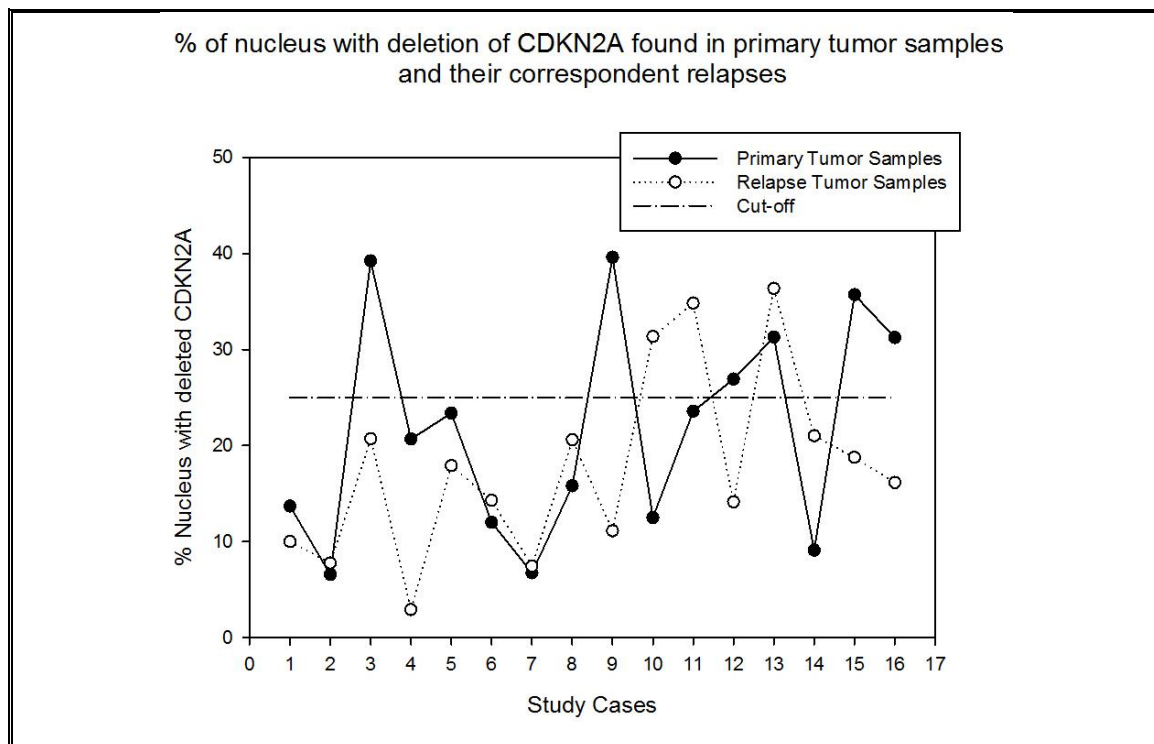


Figure 22 - Percentage of *CDKN2A* deletions in primary tumor samples vs. relapses.

Primary	Diagnosis	% CDKN2A nucleus with deletion	Relapse	Diagnosis	% CDKN2A nucleus with deletion
1	Oligodendrogliomas	13,68	2	Oligodendrogliomas	10,00
3	Oligodendrogliomas	6,56	4	Oligodendrogliomas	7,76
5	Oligodendrogliomas	39,22	6	Oligodendrogliomas	20,71
7	Oligodendrogliomas	20,68	8	Oligodendrogliomas	2,92
9	Oligoastrocytomas	23,38	10	Oligodendrogliomas	17,89
11	Astrocytomas	12,00	12	Oligodendrogliomas	14,29
13	Astrocytomas	6,74	14	Astrocytomas	7,43
15	Oligodendrogliomas	15,79	16	Oligodendrogliomas	20,59
17	Oligoastrocytomas	39,60	18	Oligodendrogliomas	11,11
19	Astrocytomas	12,50	20	Astrocytomas	31,34
21	Oligodendrogliomas	23,58	22	Oligodendrogliomas	34,83
23	Oligodendrogliomas	26,92	24	Oligoastrocytomas	14,12
25	Oligodendrogliomas	31,29	26	Oligodendrogliomas	36,36
27	Astrocytomas	9,09	28	Astrocytomas	21,01
29	Astrocytomas	35,71	30	Gliossarcoma	18,75
31	Astrocytomas	31,25	32	Astrocytomas	16,13

Figure 23 - FISH results for *CDKN2A* deletion.

The following table (Table 8) summarizes the differences found between both groups for each marker:

Table 8 - Summary of differences found in markers studied between primary tumors and relapse tumors.

Markers		Primary Tumor (P)		Relapse Tumor (R)		Variance (R –P)
		Mean	Standard Deviation	Mean	Standard Deviation	
KI-67 expression (%)		4,99	3,64	7,05	4,34	2,06
Olig-2 expression (%)		48,52	23,57	40,50	25,58	-8,02
IDH1 mut (Pixels)		5052,63	10116,73	9799,00	24383,90	4746,38
WT IDH1 (Pixels)		671939,00	180448,00	609653,00	284091,00	-62286,00
ATRX loss (Pixels)		398233,75	209797,66	354239,81	258052,35	-43993,90
EGFR (%)	4 copies	2,63	2,88	2,96	4,32	0,32
	>4 copies	4,86	4,31	6,26	6,31	1,40
	clusters	2,23	2,71	3,31	3,41	1,08
CDKN2A deletion (%)		21,75	11,35	17,83	9,69	-3,92
p53 mutation (%)		17,90	8,29	17,68	10,17	-0,22
PTEN loss (%)		7,72	3,07	7,07	3,15	-0,64
1p (%)		12,65	11,44	12,27	10,40	-0,38
19q (%)		15,88	15,21	14,19	9,27	-1,69

6. Discussion and conclusions

Diffuse gliomas are generally characterized by infiltration of the surrounding brain tissue, fact that originates fast progression and relapses.[64]

The role of individual oncogenes and tumor suppressors in the initiation of low-grade gliomas remains poorly understood.

Several lines of evidence support the notion that the *IDH1* mutation is the inciting oncogenic hit in LGG.[65]

Johnson *et al.*, through exome sequencing of *IDH*-mutated AT at initial diagnosis and recurrence showed that, while the *IDH1* is preserved, distinct clonal mutations in *P53* and *ATRX* emerge at recurrence.[66]

Similarly, our general analysis detected 4 cases in which *p53* mutations appeared in relapses and 8 cases which lost *ATRX* gene, as stressed by that author, "...the recurrent tumor contained driver mutations in *TP53* and *ATRX* distinct from those observed in the initial tumor".[66]

It is thought that expression of mutant *IDH1* alone in progenitor cells leads to pre-tumorigenic changes.[65]

Also, loss of *ATRX* by itself in a wild-type *p53* background does not lead to brain tumor formation. Likewise, *p53* loss in brain cells does not result in tumor formation by itself, unless other oncogenes are introduced.[65] Modrek *et al.* propose that the most likely order of the 3 oncogenic hits is *IDH* mutation, followed by loss of *p53* and finally loss of *ATRX*.

In literature, 3 distinct lines of mutation-based tumors (Figure 25) have been distinguished.[67] Our analysis of these 3 groups suggests that timeline of mutations may be variable –

Indeed we show tumors with *p53* mutations and *1p19q* co-deletions that keep WT *IDH1*, while *IDH1* mutation has been described to be the putative first event in gliomas' oncogenesis.

In one study, nearly all lower-grade gliomas with *IDH* mutations and no *1p/19q* co-deletion had mutations in *p53* (94%) and *ATRX* inactivation (86%). [31]

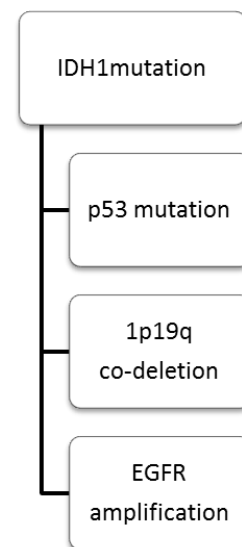


Figure 24 - Three lines of mutations-based tumors

According to our analysis, all lower-grade gliomas with *IDH* mutations and no *1p/19q* co-deletion had a relatively high percentage of *ATRX* loss, but *p53* values for mutation were low.

As expected, in our series, relapse tumors showed higher values of *KI-67*, meaning a higher cellular proliferation, while primary tumors displayed lower values.

Olig-2, which marks oligodendrocyte lineage genes expressed in glial cells, showed practically inverted results, with the higher values in primary tumors. This fact was also expected since tumors tend to loose differentiation with malignance progression.

Areas of *IDH1+ATRX-* found in both groups – primaries (low-grade) and relapses (higher grade) – are very similar, however the second group presents higher area values, meaning more tumoral cells with *IDH1* mutation and *ATRX* loss. As presented above, 56% of primary tumors without *IDH1* mutation developed this expression in their correspondent relapses, which raises the question if first tumour mutation went undetected, either by limitations of neuropathological examination or incomplete resection at surgery.

The results may show that oncogenic progression is based on such mutated cells. The identification of such a cell type may be important to establish aggressiveness of primary tumours in a diagnostic context.

As said, mutations of *IDH* and *ATRX* occur in early stage of gliomagenesis and characterize specific subtypes of gliomas in adults.[67]

IDH1 mutation has been shown to play an important role in the process of angiogenesis, cell survival and proliferation. Although this mutation would promote tumor growth, it commonly indicates a favourable prognosis independent of WHO grades.[67]

ATRX loss was recently identified as a potent biomarker in grade II-III gliomas and was associated with recurrency.[67]

Regarding *IDH1+ATRX* expression in primary tumors and relapses, sampling could play a factor in the observed results. Tumours were included in the study only if recurrence existed. Boots-Sprenger *et al.* and Xin, H. *et al.* demonstrate the favourable outcome of *1p19q* deletion, meaning the inclusion criteria could easily bias the identification of such co-deletion.[38, 68]

Bortolotto *et al.* studied *CDKN2A* homozygous deletion in 25 cases of OLG and found 8 positive cases. It was showed that *CDKN2A* did not correlate with histological grading; however, it showed a significant correlation with survival, supporting the hypothesis of an important role of this gene in prognosis of OLG.

Our results corroborate these findings. We identified 6 cases with deletions in low-grade gliomas and only 3 in higher-grade gliomas, supporting that there is no correlation with histological grading. *CDKN2A* was deleted in both groups in only 1 sample. *CDKN2A* deletion is strongly associated with poorer overall survival in AT but not in OLG or OLGA. We found deletion of *CDKN2A* in both AT and OLG/OLGA.

Molecular classification of AT by *IDH* mutation, *p53* mutation, and/or *ATRX* loss of expression revealed that *CDKN2A* loss in *IDH/p53* mutated tumours was strongly associated with worse overall survival. *CDKN2A* loss in *IDH* mutated tumors with *ATRX* loss was only weakly associated with worse overall survival.[58]

Sibin *et al* refers many studies including previous studies from his lab indicated that alterations in p16 gene and its expression are common in glioma and the *CDKN2A/B rs4977756* polymorphism shows obvious increase in the risk of glioma in Caucasians.[69] Our results are based on deletions of the *CDKN2A* gene. Gene analysis may identify not only deletions but structural changes that determine *CDKN2A* influence in tumour progression. Therefore, *CDKN2A* is associated with bad prognosis and usually presents low values. *P16* analysis would be important to identify gene alterations other than deletions, in which FISH technique is based. The use of *p16* immunohistochemistry could have valuable prognostic factor.

Percentage of *CDKN2A* deletion decreased in relapses: 8 of the 16 samples presented a deletion above 25% and 6 of which were primary tumors.

These results may suggest this gene could be related with gliomas' aggressiveness and this may be a key-marker in determining the prognosis of LGG.

The alteration of certain other well-known pro-oncogenes and tumor-suppressor genes in patients with AOLG was identified, such as mutations in phosphatidylinositol 3-kinase (*PI3K*), amplification of *EGFR* or loss of *PTEN* tumor suppressor.[70] *EGFR* gene amplification and overexpression are rare in low-grade gliomas but are very typical in GB.[43-44]

Our data showed *EGFR* amplification in about one fifth of the samples. These results are supporting the findings described. There was 1 case with amplification exclusively in the primary tumor. Those values seem almost virtually equal and this difference is probably related to the sampling location.

Nevertheless, lower percentages of *PTEN* deletions were found in our samples, suggesting this marker is probably not one of the key-markers in gliomas'

aggressiveness. Similar results were found for p53, interestingly both being the main tumor suppressors mutated in most solid cancers.

In conclusion, the differences in the populations (*IDH1mut/ATRXloss*, *IDH1mut/ATRX/1p/19q* co-del and *IDH1wt*) between primary tumor samples and their relapses studied by us, are subtle and perhaps biological drive towards malignancy cannot be distinguished using these markers alone.

We did find differences in genetic and immunohistochemical markers, mainly: *Ki-67*, *Olig-2*, *EGFR* and *CDKN2A*. [67, 69] Our samples showed multiple genetic events and led us to think tumour relapses need to be studied with clinical data, especially survival that might allow a clearer view of distinguishable paths towards oncogenicity. We found differences in some putative oncogenic pathways. Relapses seem, when considered as whole entity, to have proliferation and oncogenic pathways, like *EGFR*, different from the original tumour, howbeit small in number.

The reduced number of cases is a limitation to this study. Also, FISH analysis in TMA samples instead of the whole extension of the tumors was a limitation as well, and this decision was linked to the lack of time necessary to perform such time consuming technique. Our choices tried to overcome such limitations, since the sample size is considerable, based in our bibliographic search. FISH was performed at tumour site, choosing tumour cells that were representative of the whole tumour. Extensive genetic analysis, ideally next generation sequencing, could not be performed but would complement our findings with a clearer genetic profile of low grade gliomas in our population.

It should be interesting to continue this line of research, comparing primary tumors with their own relapses, since there are very few papers published with similar cases; perhaps using DNA sequencing instead of FISH techniques, and comparing the results with real survival rates and patient outcomes.

The objective is not just to characterise histological subgroups of gliomas, but also to try to understand what protein or genetic component in the tumor is responsible for the relapse in a much more aggressive form. Predicting such behaviour could mean better chances of controlling the progression of the disease right in the moment of the first diagnosis.

7. References

- [1] J. Ruiz and G. Lesser, “Low-grade gliomas,” *Curr Treat Options Oncol*, vol. 10, no. 3–4, pp. 231–42, 2009.
- [2] S. F. Malheiros, J. N. Stávale, C. M. Franco, F. M. Braga, and A. A. Gabbai, “Astrocitomas Difusos de Baixo Grau de Malignidade,” *Rev. Neurociências*, vol. 6, no. 2, pp. 75–80, 1998.
- [3] M. J. Riemenschneider, J. W. M. Jeuken, P. Wesseling, and G. Reifenberger, “Molecular diagnostics of gliomas: state of the art,” *Acta Neuropathol*, no. 120, pp. 567–584, 2010.
- [4] D. N. Louis *et al.*, “The 2016 World Health Organization Classification of Tumors of the Central Nervous System: a summary,” *Acta Neuropathol.*, vol. 131, no. 6, pp. 803–820, 2016.
- [5] S. Brandner and A. von Deimling, “Review: Diagnostic, prognostic and predictive relevance of molecular markers in gliomas,” *Neuropathol. Appl. Neurobiol.*, p. n/a-n/a, 2015.
- [6] P. O. Guichet *et al.*, “Asymmetric distribution of GFAP in glioma multipotent cells,” *PLoS One*, vol. 11, no. 3, pp. 1–13, 2016.
- [7] I. F. Tsigelny *et al.*, “Molecular mechanisms of OLIG2 transcription factor in brain cancer,” *Oncotarget*, vol. 5, no. 0, 2016.
- [8] S. Ghasimi *et al.*, “Genetic risk variants in the CDKN2A/B, RTEL1 and EGFR genes are associated with somatic biomarkers in glioma,” *J. Neurooncol.*, vol. 127, no. 3, pp. 483–492, 2016.
- [9] A. Korshunov, R. Sycheva, and A. Golanov, “The prognostic relevance of molecular alterations in glioblastomas for patients age < 50 years,” *Cancer*, no. 104 (4), pp. 825–832, 2005.
- [10] J. Smith, I. Tachibana, and S. et al Passe, “PTEN mutation, EGFR amplification, and outcome in patients with anaplastic astrocytoma and glioblastoma multiforme,” *J Natl Cancer Inst.*

- [11] D. Williams Parsons *et al.*, “An Integrated Genomic Analysis of Human Glioblastoma Multiforme.”
- [12] T. Watanabe, S. Nobusawa, P. Kleihues, and H. Ohgaki, “IDH1 Mutations Are Early Events in the Development of Astrocytomas and Oligodendrogliomas.”
- [13] M. Sanson *et al.*, “Isocitrate dehydrogenase 1 codon 132 mutation is an important prognostic biomarker in gliomas,” *J. Clin. Oncol.*, vol. 27, no. 25, pp. 4150–4, Sep. 2009.
- [14] M. R. Kang *et al.*, “Mutational analysis of IDH1 codon 132 in glioblastomas and other common cancers,” *Int. J. Cancer*, vol. 125, no. 2, pp. 353–355, Jul. 2009.
- [15] A. L. Cohen, S. L. Holmen, and H. Colman, “IDH1 and IDH2 mutations in gliomas,” *Curr. Neurol. Neurosci. Rep.*, vol. 13, no. 5, p. 345, May 2013.
- [16] H. Yan *et al.*, “IDH1 and IDH2 Mutations in Gliomas,” *Neuro. Oncol.*
- [17] X. Xu *et al.*, “Structures of human cytosolic NADP-dependent isocitrate dehydrogenase reveal a novel self-regulatory mechanism of activity,” *J. Biol. Chem.*, vol. 279, no. 32, pp. 33946–57, Aug. 2004.
- [18] M. S. Waitkus, B. H. Dillas, and H. Yan, “Isocitrate dehydrogenase mutations in gliomas,” *Neuro. Oncol.*, vol. 18, no. 1, pp. 16–26, 2016.
- [19] H. Yan, D. D. Bigner, V. Velculescu, and D. W. Parsons, “Mutant metabolic enzymes are at the origin of gliomas,” *Cancer Res.*, vol. 69, no. 24, pp. 9157–9, Dec. 2009.
- [20] J.-P. Bayley and P. Devilee, “Warburg tumours and the mechanisms of mitochondrial tumour suppressor genes. Barking up the right tree?,” *Curr. Opin. Genet. Dev.*, vol. 20, no. 3, pp. 324–329, Jun. 2010.
- [21] T. C. Pansuriya *et al.*, “Somatic mosaic IDH1 or IDH2 mutations are associated with enchondroma and spindle cell hemangioma in Ollier disease and Maffucci syndrome.”
- [22] M. E. Figueroa *et al.*, “Leukemic IDH1 and IDH2 mutations result in a hypermethylation phenotype, disrupt TET2 function, and impair hematopoietic

differentiation.”

- [23] R. J. Gibbons, D. J. Picketts, L. Villard, and D. R. Higgs, “Mutations in a Putative Global Transcriptional Regulator Cause X-Linked Mental Retardation with α -Thalassemia (ATR-X Syndrome),” *Cell*, vol. 80, pp. 837–845, 1995.
- [24] M. J. Law *et al.*, “ATR-X Syndrome Protein Targets Tandem Repeats and Influences Allele-Specific Expression in a Size-Dependent Manner,” *Cell*, vol. 143, no. 3, pp. 367–378, Oct. 2010.
- [25] K. Ritchie, C. Seah, J. Moulin, C. Isaac, F. Dick, and N. G. Bérubé, “Loss of ATRX leads to chromosome cohesion and congression defects,” *J. Cell Biol.*, vol. 180, no. 2, pp. 315–324, Jan. 2008.
- [26] D. J. Picketts, D. R. Higgs, S. Bachoo, D. J. Blake, O. W. Quarrell, and R. J. Gibbons, “ATR-X encodes a novel member of the SNF2 family of proteins: mutations point to a common mechanism underlying the ATR-X syndrome,” *Hum. Mol. Genet.*, vol. 5, no. 12, pp. 1899–907, Dec. 1996.
- [27] Y. Xue *et al.*, “The ATRX syndrome protein forms a chromatin-remodeling complex with Daxx and localizes in promyelocytic leukemia nuclear bodies,” *Proc. Natl. Acad. Sci. U. S. A.*, vol. 100, no. 19, pp. 10635–40, Sep. 2003.
- [28] J. Tang *et al.*, “A novel transcription regulatory complex containing death domain-associated protein and the ATR-X syndrome protein,” *J. Biol. Chem.*, vol. 279, no. 19, pp. 20369–77, May 2004.
- [29] T. L. McDowell *et al.*, “Localization of a putative transcriptional regulator (ATR-X) at pericentromeric heterochromatin and the short arms of acrocentric chromosomes,” *Proc. Natl. Acad. Sci. U. S. A.*, vol. 96, no. 24, pp. 13983–8, Nov. 1999.
- [30] D. P. Steensma, R. J. Gibbons, and D. R. Higgs, “Acquired α -thalassemia in association with myelodysplastic syndrome and other hematologic malignancies,” *Blood*, vol. 105, no. 2, pp. 443–52, 2005.
- [31] Cancer Genome Atlas Research Network *et al.*, “Comprehensive, Integrative Genomic Analysis of Diffuse Lower-Grade Gliomas,” *N. Engl. J. Med.*, vol.

- 372, no. 26, pp. 2481–98, Jun. 2015.
- [32] K. Kannan *et al.*, “Whole-exome sequencing identifies ATRX mutation as a key molecular determinant in lower-grade glioma,” *Oncotarget*, vol. 3, no. 10, pp. 1194–203, Oct. 2012.
 - [33] W. Biernat, Y. Tohma, Y. Yonekawa, P. Kleihues, and H. Ohgaki, “Alterations of cell cycle regulatory genes in primary (de novo) and secondary glioblastomas,” *Acta Neuropathol.*, vol. 94, no. 4, pp. 303–9, Oct. 1997.
 - [34] S. H. Bigner *et al.*, “Relationship between gene amplification and chromosomal deviations in malignant human gliomas,” *Cancer Genet. Cytogenet.*, vol. 29, no. 1, pp. 165–70, Nov. 1987.
 - [35] J. Reifenberger, G. Reifenberger, L. Liu, C. D. James, W. Wechsler, and V. P. Collins, “Molecular genetic analysis of oligodendroglial tumors shows preferential allelic deletions on 19q and 1p,” *Am. J. Pathol.*, vol. 145, no. 5, pp. 1175–90, Nov. 1994.
 - [36] J. G. Cairncross *et al.*, “Specific genetic predictors of chemotherapeutic response and survival in patients with anaplastic oligodendrogliomas,” *J. Natl. Cancer Inst.*, vol. 90, no. 19, pp. 1473–9, Oct. 1998.
 - [37] J. M. Kros *et al.*, “Panel review of anaplastic oligodendroglioma from European Organization For Research and Treatment of Cancer Trial 26951: assessment of consensus in diagnosis, influence of 1p/19q loss, and correlations with outcome,” *J. Neuropathol. Exp. Neurol.*, vol. 66, no. 6, pp. 545–51, Jun. 2007.
 - [38] S. H. E. Boots-Sprenger *et al.*, “Significance of complete 1p/19q co-deletion, IDH1 mutation and MGMT promoter methylation in gliomas: Use with caution,” *Mod. Pathol.*, vol. 26, no. 7, pp. 922–929, 2013.
 - [39] S. B. Wharton *et al.*, “Subtypes of oligodendroglioma defined by 1p,19q deletions, differ in the proportion of apoptotic cells but not in replication-licensed non-proliferating cells,” *Acta Neuropathol.*, vol. 113, no. 2, pp. 119–27, Feb. 2007.
 - [40] M. B. Murphrey and S. S. Bhimji, *Biochemistry, Epidermal Growth Factor*

Receptor. StatPearls Publishing, 2018.

- [41] P. H. Huang, A. M. Xu, and F. M. White, “Oncogenic EGFR Signaling Networks in Glioma,” *Sci. Signal.*, vol. 2, no. 87, pp. re6-re6, Sep. 2009.
- [42] B. Mukherjee *et al.*, “EGFRvIII and DNA double-strand break repair: a molecular mechanism for radioresistance in glioblastoma,” *Cancer Res.*, vol. 69, no. 10, pp. 4252–9, May 2009.
- [43] M. Nagane, F. Coufal, H. Lin, O. Böglér, W. K. Cavenee, and H. J. Huang, “A common mutant epidermal growth factor receptor confers enhanced tumorigenicity on human glioblastoma cells by increasing proliferation and reducing apoptosis,” *Cancer Res.*, vol. 56, no. 21, pp. 5079–86, Nov. 1996.
- [44] J. Li, R. Liang, C. Song, Y. Xiang, and Y. Liu, “Prognostic significance of epidermal growth factor receptor expression in glioma patients,” *Onco. Targets. Ther.*, vol. Volume 11, pp. 731–742, 2018.
- [45] K. J. Hatanpaa, S. Burma, D. Zhao, and A. A. Habib, “Epidermal Growth Factor Receptor in Glioma: Signal Transduction, Neuropathology, Imaging, and Radioresistance,” *Neoplasia*, vol. 12, no. 9, pp. 675–684, 2010.
- [46] J. A. Boockvar *et al.*, “Constitutive EGFR signaling confers a motile phenotype to neural stem cells,” *Mol. Cell. Neurosci.*, vol. 24, no. 4, pp. 1116–30, Dec. 2003.
- [47] J. Li *et al.*, “PTEN, a putative protein tyrosine phosphatase gene mutated in human brain, breast, and prostate cancer,” *Science*, vol. 275, no. 5308, pp. 1943–7, Mar. 1997.
- [48] D. C. I. Gobarahan and C. Wilson, “PTEN: tumour suppressor, multifunctional growth regulator and more,” *Hum. Mol. Genet.*, vol. 12 Spec No, no. suppl 2, pp. R239–48, Oct. 2003.
- [49] C. Eng, “PTEN: One Gene, Many Syndromes,” *Hum. Mutat.*, vol. 22, no. 3, pp. 183–198, Sep. 2003.
- [50] H. Sasaki, M. C. Zlatescu, R. A. Betensky, Y. Ino, J. G. Cairncross, and D. N. Louis, “PTEN is a target of chromosome 10q loss in anaplastic

- oligodendrogliomas and PTEN alterations are associated with poor prognosis.,” *Am. J. Pathol.*, vol. 159, no. 1, pp. 359–67, Jul. 2001.
- [51] R. T. Mott, K. C. Turner, D. D. Bigner, and R. E. McLendon, “Utility of *EGFR* and *PTEN* numerical aberrations in the evaluation of diffusely infiltrating astrocytomas,” *J. Neurosurg.*, vol. 108, no. 2, pp. 330–335, Feb. 2008.
 - [52] J. A. Benitez *et al.*, “ARTICLE PTEN regulates glioblastoma oncogenesis through chromatin-associated complexes of DAXX and histone H3.3,” *Nat. Commun.*, vol. 8, 2017.
 - [53] W. Hong Shen *et al.*, “Essential Role for Nuclear PTEN in Maintaining Chromosomal Integrity.”
 - [54] M. Ruas and G. Peters, “The p16INK4a/CDKN2A tumor suppressor and its relatives.,” *Biochim. Biophys. Acta*, vol. 1378, no. 2, pp. F115-77, Oct. 1998.
 - [55] J. Boström *et al.*, “Alterations of the tumor suppressor genes CDKN2A (p16(INK4a)), p14(ARF), CDKN2B (p15(INK4b)), and CDKN2C (p18(INK4c)) in atypical and anaplastic meningiomas.,” *Am. J. Pathol.*, vol. 159, no. 2, pp. 661–9, Aug. 2001.
 - [56] R. Cement, “(Câncer de Próstata).”
 - [57] N. F. Schlecht *et al.*, “Epigenetic changes in the CDKN2A locus are associated with differential expression of P16INK4A and P14ARF in HPV-positive oropharyngeal squamous cell carcinoma,” *Cancer Med.*, vol. 4, no. 3, pp. 342–353, 2015.
 - [58] S. Bortolotto *et al.*, “CDKN2A/p16 inactivation in the prognosis of oligodendrogliomas.,” *Int. J. cancer*, vol. 88, no. 4, pp. 554–7, Nov. 2000.
 - [59] C. T. Rueden *et al.*, “ImageJ2: ImageJ for the next generation of scientific image data,” *BMC Bioinformatics*, vol. 18, no. 18, 2017.
 - [60] A. C. Ruifrok and D. A. Johnston, “Quantification of histochemical staining by color deconvolution.,” *Anal. Quant. Cytol. Histol.*, vol. 23, no. 4, pp. 291–9, Aug. 2001.

- [61] V. J. Tuominen, S. Ruotoistenmäki, A. Viitanen, M. Jumppanen, and J. Isola, "ImmunoRatio: a publicly available web application for quantitative image analysis of estrogen receptor (ER), progesterone receptor (PR), and Ki-67," *Breast Cancer Res.*, vol. 12, no. 4, p. R56, Aug. 2010.
- [62] R. Vijayashree, P. Aruthra, and K. R. Rao, "A Comparison of Manual and Automated Methods of Quantitation of Oestrogen/Progesterone Receptor Expression in Breast Carcinoma," *J. Clin. DIAGNOSTIC Res.*, vol. 9, no. 3, pp. EC01-5, Mar. 2015.
- [63] S. H. Arif Arshad A *et al.*, "EGFR and PTEN Gene Mutation Status in Glioblastoma Patients and their Prognostic Impact on Patient's Survival," *J. Carcinog. Mutagen.*, vol. 06, no. 02, pp. 1–7, Mar. 2015.
- [64] C. Lauber, B. Klink, and M. Seifert, "Comparative analysis of histologically classified oligodendrogliomas reveals characteristic molecular differences between subgroups.," *BMC Cancer*, vol. 18, no. 1, p. 399, Apr. 2018.
- [65] A. S. Modrek *et al.*, "Low-Grade Astrocytoma Mutations in IDH1, P53, and ATRX Cooperate to Block Differentiation of Human Neural Stem Cells via Repression of SOX2.," *Cell Rep.*, vol. 21, no. 5, pp. 1267–1280, Oct. 2017.
- [66] B. E. Johnson *et al.*, "Mutational Analysis Reveals the Origin and Therapy-Driven Evolution of Recurrent Glioma," *Science (80-.)*, vol. 343, no. 6167, pp. 189–193, Jan. 2014.
- [67] J. Cai, P. Zhu, C. Zhang, Q. Li, and Z. Wang, "Detection of ATRX and IDH1-R132H immunohistochemistry in the progression of 211 paired gliomas," vol. 7, no. 13, pp. 16384–16395, 2007.
- [68] X. Hu *et al.*, "Multigene signature for predicting prognosis of patients with 1p19q co-deletion diffuse glioma," *Neuro. Oncol.*, vol. 19, no. 6, pp. 786–795, Jun. 2017.
- [69] M. K. Sibin *et al.*, "Two gene polymorphisms (rs4977756 and rs11515) in CDKN2A/B and glioma risk in South Indian population.," *Meta gene*, vol. 9, pp. 215–8, Sep. 2016.

- [70] J. Polivka *et al.*, “Co-deletion of 1p/19q as Prognostic and Predictive Biomarker for Patients in West Bohemia with Anaplastic Oligodendroglioma.”, *Anticancer Res.*, vol. 36, no. 1, pp. 471–6, Jan. 2016.

8.1 Appendix 1: IHC technique protocol

1. Dewax and hydration
2. Endogenous peroxidase inhibition – 3% - 10m
3. Antigen retrieval – H3300 vector citrate buffer (9,375mL to 1L H₂O), Microwave: 600W/10m + 850W/20m
4. Cooling and assembling on Sequenza with PBS buffer
5. Rinse with PBS
6. Incubation of primary antibody – ON at 4°C
7. Rinse twice with PBS
8. Incubation of secondary antibody – 1hour at RT
9. Rinse twice with PBS
10. Disassemble and revelation with DAB – 5m
11. Rinse in tap water
12. Counterstain in Harris Hematoxylin – 4m
13. Rinse in tap water
14. Differentiate in 1% hydrochloric alcohol
15. Rinse in tap water
16. Blue with 1% ammoniacal water
17. Rinse in tap water
18. Dehydrate, clear and mount with mounting media

8.2 Appendix 2: FISH technique protocol

1. Dewax and hydration
2. Antigen retrieval – H3300 vector citrate buffer (9,375mL to 1L H₂O), Microwave: 600W/10m + 850W/20m
3. Pre-hybridization solution – sodium thiocyanate – 82°C/10m
4. Ethanol
5. Digestion solution – pepsin – 37°C/10m
6. Ethanol
7. Air Dry
8. Incubate the probes in the slides and cover with the coverslips
9. Place slides on the hybridizer and define programme (60min between 55° - 62°C; 2min at 95°C; ON at 37°C)
10. Post-hybridization solution I – 10m (or until the coverslips fall out)
11. Post-hybridization solution II – 75°C/3 seconds with agitation
12. Rinse in distilled water
13. Counterstain with DAPI – 2m
14. Dehydrate, clear and mount with mounting media

8.3 Appendix 3: EGFR FISH results

Primary	Diagnosis	% EGFR CLUSTERS	% EGFR 4 COPIES	%EGFR > 4 COPIES	Relapse	Diagnosis	% EGFR CLUSTERS	% EGFR 4 COPIES	%EGFR > 4 COPIES
1	Oligodendrogliomas	0,00	2,86	2,86	2	Oligodendrogliomas	0,85	0,00	0,85
3	Oligodendrogliomas	4,55	0,00	4,55	4	Oligodendrogliomas	0,90	2,70	3,60
5	Oligodendrogliomas	2,50	0,00	2,50	6	Oligodendrogliomas	1,67	0,00	1,67
7	Oligodendrogliomas	0,91	1,82	2,73	8	Oligodendrogliomas	2,19	2,19	4,38
9	Oligoastrocytomas	0,00	0,00	0,00	10	Oligodendrogliomas	3,97	0,79	4,76
11	Astrocytomas	0,00	5,71	5,71	12	Oligodendrogliomas	4,65	9,30	13,95
13	Astrocytomas	6,06	9,09	15,15	14	Astrocytomas	4,00	9,71	13,71
15	Oligodendrogliomas	0,00	6,52	6,52	16	Oligodendrogliomas	5,43	5,43	10,85
17	Oligoastrocytomas	0,00	0,00	0,00	18	Oligodendrogliomas	0,00	0,00	0,00
19	Astrocytomas	4,76	4,76	9,52	20	Astrocytomas	13,04	0,00	13,04
21	Oligodendrogliomas	7,41	2,22	9,63	22	Oligodendrogliomas	1,79	1,79	3,57
23	Oligodendrogliomas	3,45	5,75	9,20	24	Oligoastrocytomas	0,00	0,56	0,56
25	Oligodendrogliomas	0,00	1,67	1,67	26	Oligodendrogliomas	0,00	0,00	0,00
27	Astrocytomas	0,00	0,00	0,00	28	Astrocytomas	7,30	13,87	21,17
29	Astrocytomas	6,00	0,00	6,00	30	gliosarcoma	5,17	0,00	5,17
31	Astrocytomas	0,00	1,74	1,74	32	Astrocytomas	1,92	0,96	2,88

8.4 Appendix 4: p53 FISH results

Primary	Diagnosis	p53 mutation	Relapse	Diagnosis	p53 mutation
1	Oligodendrogliomas	17,33	2	Oligodendrogliomas	10,34
3	Oligodendrogliomas	15,38	4	Oligodendrogliomas	10,64
5	Oligodendrogliomas	12,00	6	Oligodendrogliomas	8,39
7	Oligodendrogliomas	10,74	8	Oligodendrogliomas	34,21
9	Oligoastrocytomas	20,74	10	Oligodendrogliomas	6,80
11	Astrocytomas	23,26	12	Oligodendrogliomas	16,98
13	Astrocytomas	16,09	14	Astrocytomas	13,20
15	Oligodendrogliomas	12,50	16	Oligodendrogliomas	20,96
17	Oligoastrocytomas	43,88	18	Oligodendrogliomas	22,95
19	Astrocytomas	20,00	20	Astrocytomas	11,76
21	Oligodendrogliomas	14,40	22	Oligodendrogliomas	10,68
23	Oligodendrogliomas	9,90	24	Oligoastrocytomas	37,29
25	Oligodendrogliomas	14,20	26	Oligodendrogliomas	26,39
27	Astrocytomas	12,34	28	Astrocytomas	12,95
29	Astrocytomas	17,39	30	gliosarcoma	6,67
31	Astrocytomas	26,25	32	Astrocytomas	32,63